

**Application of Synchrophasors for Validation of  
Transmission Line Distance Relay Parameters**

A Dissertation

Presented in Partial Fulfillment of the Requirements for the

Degree of Doctorate of Philosophy

with a

Major in Electrical Engineering

in the

College of Graduate Studies

University of Idaho

by

Salah Eddine Jadid

December 2014

Major Professor: Brian K. Johnson, Ph.D.



## Abstract

Synchrophasors, defined as synchronized phasors, provide a real-time measurement of electrical quantities from across the power system. Applications include wide-area control, system model validation, determining stability margins, maximizing stable system loading, islanding detection, system-wide disturbance recording, and visualization of dynamic system response.

This research utilized synchrophasor technology, which takes measurements at both ends of the line to validate transmission line distance relay settings. Methods were developed for the calculation of transmission line parameters, specifically the positive-sequence and zero-sequence impedance of the line for both transposed and untransposed transmission lines. In the case of parallel lines, in addition to the positive- and zero-sequence impedance of the line, the zero-sequence mutual coupling was derived. For the case of transposed lines, a comparison between the Pi equivalent circuit and distributed parameter lines showed no significant difference between the two methods.

PSCAD<sup>™</sup>/EMTDC<sup>™</sup> simulations were used to validate and verify the performance of the proposed method for the calculation of the transmission line parameters. Also, field data from Entergy phasor measurement units (PMUs) on a transmission line was presented. The calculation from the field measured data was calculated with actual relay settings and a method was proposed for validating the relay settings.

A Real Time Digital Simulator (RTDS<sup>®</sup>), GPS satellite-synchronized clock, PMUs, phasor data concentrators (PDCs), communications equipment, and visualization software were used

to set up a network and simulate various cases to verify the performance and further validate the results.

## **Acknowledgements**

This has been a long road that would not have been possible without support from the faculty at the University of Idaho and especially my major professor Dr. Brian Johnson. He has constantly gone above and beyond on behalf of my education and provided great support throughout the years. He mentors me by inspiring and encouraging and gives me the freedom to do what I am excited to do in my field and helps me succeed. It was such a pleasant experience to work with Dr. Brian. He is my lifetime mentor and friend. I would like to thank my committee members for their time, support, and academic knowledge throughout the classes I've taken during my Ph.D. studies. I would also like to acknowledge the assistance of graduate assistant Alaap Anujan. He made the connection to the lab equipment used in this research and made sure that it was wired properly. Above all, none of this would have been possible without the support of my wife, Natalie, and my two boys, Adam and Sammy. Their support and encouragement allowed me to complete my research.

## **Dedication**

To my parents.

## Table of Contents

Authorization to Submit Dissertation.....	ii
Abstract .....	iii
Acknowledgements .....	v
Dedication .....	vi
Table of Contents .....	vii
List of Tables .....	x
List of Figures .....	xi
List of Abbreviations .....	xiv
Introduction.....	1
Chapter 1 Review of Key Concepts and Literature.....	4
1.1 Software Tools.....	4
1.2 Impedance Measurements Using Test Equipment .....	6
1.3 Methods for the Calculation of Transmission Line Impedance .....	7
1.4 Relay Settings Overview .....	9
1.4.1 Zone Distance Settings.....	10
1.4.2 Ground Distance Elements.....	11
1.4.3 Zero-Sequence Compensation Factor .....	12
Chapter 2 Transmission Line Theory and Modeling.....	13
2.1 Overview of the Transmission Line Parameter Calculation.....	13
2.1.1 Transmission Line Series Impedance.....	13
2.1.2 Transmission Line Shunt Admittance Matrix .....	19
2.2 Transmission Line Modeling.....	21
2.3 Synchrophasors Overview .....	23
2.4 Transposed Lines.....	25
2.4.1 Equivalent Pi Solution Algorithm.....	25
2.4.2 Distributed Parameter Line .....	27
2.5 Untransposed Transmission Lines.....	32
2.5.1 Equivalent PI circuit.....	32
Chapter 3 Validation of Transmission Line Relay Parameters Using Synchrophasors .....	35

3.1	Paper Abstract .....	35
3.2	Paper Introduction .....	35
3.3	Line Modeling .....	38
3.3.1	Equivalent PI Circuit.....	40
3.3.2	Steady-State Distributed Line Parameters .....	41
3.3.3	Classification of Transmission Lines .....	42
3.4	Calculation of Parameters.....	42
3.4.1	General Overview .....	42
3.4.2	Transposed Lines .....	43
3.4.3	Untransposed Lines.....	45
3.5	Case Study.....	47
3.6	Case Study Results and Discussion.....	50
3.7	Conclusion.....	59
3.8	Comments.....	60
Chapter 4	RTDS Validation Testing .....	62
4.1	Test Setup .....	62
4.2	RTDS and Power System Overview .....	63
4.2.1	RTDS Overview.....	63
4.2.2	Power System Overview .....	64
4.3	Configuration and Description of the Network Equipment .....	65
4.3.1	Description of the Synvphasor.....	65
4.3.2	SEL-421 Global Settings .....	66
4.3.3	Port 5 settings.....	67
4.3.4	Phasor Data Concentrator .....	68
4.3.5	Description of the SEL-5073 PDC.....	68
4.3.6	Settings for the SEL-5073 .....	69
4.4	Verification of the Test System During Steady State.....	73
4.5	RTDS Test Results .....	80
4.5.1	Transposed Lines .....	81
4.5.2	Untransposed Lines.....	89
4.6	Discussion and Summary of Results .....	96



Chapter 5 Measurement of Parallel Transmission Lines Parameters.....	99
5.1 Overview of the Calculation of Parallel Transmission Line Impedance.....	99
5.2 PSCAD/EMTDC Simulation and Results.....	101
5.3 Relay Settings for Parallel Lines.....	105
Chapter 6 Conclusion and Future Work.....	108
6.1 Summary and Conclusion.....	108
6.2 Future Work.....	109
References.....	112
Appendices.....	115
Appendix A: Detail Circuit of the Power System Model.....	115
A.1 Source 1 Data.....	115
A.2 Source 2 Data.....	116
A.3 Source 3 Data.....	116
A.4 Current Transformer Data.....	116
A.5 Potential Transformer Data.....	117
Appendix B: Solving a System of Linear Equations.....	118
B.1 Mathcad Isolve and geninv functions.....	118

## List of Tables

Table 1	Line Impedance Comparison for Transposed line .....	45
Table 2	Line Impedance Comparison for Untransposed Line .....	47
Table 3	Relay Transmission Line Parameters .....	57
Table 4	Phase Distance Zone Settings .....	57
Table 5	Ground Distance Zone Settings .....	58
Table 6	Zero-Sequence Compensation Factor .....	59
Table 7	Directional Element Settings .....	59
Table 8	Results for Short Transmission Line.....	82
Table 9	Results for Medium Transmission Line.....	83
Table 10	Results for Long Transmission Line.....	84
Table 11	Results for Short Transmission Line.....	85
Table 12	Results for Medium Transmission Line.....	86
Table 13	Results for Long Transmission Line.....	87
Table 14	Results for Short Transmission Line.....	90
Table 15	Results for Medium Transmission Line.....	91
Table 16	Results for Long Transmission Line.....	92
Table 17	Results for Medium Untransposed Transmission Line No Ground Wires .....	93
Table 18	Results for Short Transmission Line.....	94
Table 19	Results for Medium Transmission Line.....	95
Table 20	Results for Long Transmission Line.....	96
Table 21	Transmission Circuit 1 Results .....	103
Table 22	Transmission Circuit 2 Results .....	104
Table 23	Zero-Sequence Mutual Coupling Results .....	105

## List of Figures

Figure 1	Aspen Model of a Transmission Line Showing Three Phases and Two Ground Wires	5
Figure 2	ASPEN Line Constants Program Screen Captures Showing the Physical Configuration of a Transmission Line	5
Figure 3	Test Set Connections for a (a) Single-Phase-to-Ground Loop Test, (b) Phase-to-Phase Loop Test, and (c) Three-Phase-to-Ground Loop Test	7
Figure 4	Overhead Transmission Line With Protection at Each End	9
Figure 5	Relay Settings for Transmission Line Parameters	10
Figure 6	Relay Settings for Mho Phase Distance Protection	11
Figure 7	Relay Settings for Mho Ground Distance Protection	12
Figure 8	Relay Settings for Zero-Sequence Compensation Factor	12
Figure 9	(a) Two-Conductor Model (b) Three-Phase System With Ground Conductor	14
Figure 10	Effect of Ground Resistivity on Zero-Sequence Impedance Magnitude	17
Figure 11	Arrangements of Image Conductors in a Three-Phase Transmission Line	19
Figure 12	Transposed Transmission Line	20
Figure 13	Equivalent PI Circuit of a Three-Phase Transmission line	22
Figure 14	Distributed Parameter Circuit of a Transmission line	22
Figure 15	Reference Wave and “Local” Wave With Angular Comparison	24
Figure 16	Equivalent Pi Diagram Showing Current Voltages and the Unknown Parameters $Z$ and $Y$	25
Figure 17	Model of a Three-Phase Transmission Line With Mutual Impedance	38
Figure 18	Equivalent PI Circuit of a Three-Phase Transmission Line	40
Figure 19	Distributed Model of a Three-Phase Transmission Line	41
Figure 20	PSCAD/EMTDC Test Setup and Model for Testing	43
Figure 21	PMU One-Line Diagram for the Case Study	48
Figure 22	PMUS Setup and Requirements	48
Figure 23	Measured Currents From the PMUs During Prefault and Post-Fault Load Conditions and the Unbalance State	49

Figure 24	Measured Voltages From the PMUs During Prefault and Post-Fault Load Conditions and the Unbalance State	49
Figure 25	Positive-Sequence Voltage Angle Difference Between the Two Stations From the PMUs During Prefault and Post-Fault Load Conditions and the Unbalance State	50
Figure 26	Comparison of the Positive-Sequence Impedance Vectors Calculated From the Three LCC Programs	51
Figure 27	Comparison of the Zero-Sequence Impedance Vectors Calculated From the Three LCC Programs	51
Figure 28	Comparison of the Positive-Sequence Impedance Vectors Calculated From the Three LCC Programs and Synchrophasors	52
Figure 29	Comparison of the Zero-Sequence Impedance Vectors Calculated From the Three LCC Programs and Synchrophasors	52
Figure 30	Comparison of the Zero-Sequence Compensation Factor Vectors Calculated From the Three LCC Programs and Synchrophasors	54
Figure 31	Per-Unit Reach Versus Phase-to-Ground Fault Current Magnitude for Calculated Zero-Sequence Compensation Factors From Entergy LCC and Synchrophasors	55
Figure 32	Experimental Network Set Up	63
Figure 33	Power System Modeled in RTDS	65
Figure 34	PMU Settings	66
Figure 35	Additional PMU Settings	67
Figure 36	Port Settings	67
Figure 37	SEL-5073 PDC Internal Architecture	68
Figure 38	PDC Input Configuration	70
Figure 39	PDC Output Configuration	72
Figure 40	PDC Archiver Configuration	73
Figure 41	Primary Currents Simulated in the RTDS	74
Figure 42	Secondary Currents Simulated in the RTDS	75
Figure 43	Primary Voltage Simulated in the RTDS	76
Figure 44	Secondary Voltages Simulated in the RTDS	76
Figure 45	PMU Metering Screen Capture	77
Figure 46	PMU Synchrophasors Values Screen Capture	78
Figure 47	PDC Screen Capture Receiving PMU Data	79

Figure 48	Visualization Software for PMU Data	80
Figure 49	Horizontal Tower Properties	81
Figure 50	Vertical Tower Properties	84
Figure 51	Horizontal Tower Configuration Results	88
Figure 52	Vertical Tower Configuration Results	89
Figure 53	Horizontal Tower Configuration Results	97
Figure 54	Vertical Tower Configuration Results	98
Figure 55	PSCAD/EMTDC Simulation Results for Steady State Load Condition	98
Figure 56	Two Parallel Transmission Lines Separated by Distance $d$	99
Figure 57	PSCAD/EMTDC Set Up for Untransposed Parallel Transmission Line	101
Figure 58	Parallel Transmission Line System One Line	106
Figure 59	CT Data	116
Figure 60	Equivalent CVT Model in RSCAD	117
Figure 61	CVT Transformer Data	117
Figure 62	CVT Burden Data	117
Figure 63	CVT Ferro-Resonance Filter Data	118

## List of Abbreviations

PMU	Phasor Measurement Unit
PSCAD	Power System Computer Aided Design
EMTDC	Electro Magnetic Transients for DC
LCC	Line Constants Calculations
RTDS	Real Time Digital Simulator
RSCAD	Real Time Simulation Computer Aided Design Software
GPS	Global Positioning Satellite System
PDC	Phasor Data Concentrator
SCADA	Supervisory Control and Data Acquisition
HMI	Human Machine Interface
Mbps	Mega Bits Per Second
SEL	Schweitzer Engineering Laboratories

## Introduction

The offline calculation of transmission line impedance has long been used by engineers to determine appropriate distance relay settings. Accurate calculation is paramount for reliable distance relay operation and correct fault location. Transmission line impedance is estimated based on the tower configuration and physical properties of the conductor. These transmission line impedance estimates are based on assumptions and approximations, such as ground resistivity and temperature. Incorrect transmission line impedance values in transmission line models can lead to inadequate relay settings that can potentially lead to distance element undesired operation. Distance relays require input of the positive-sequence ( $Z_{1L}$ ) and zero-sequence ( $Z_{0L}$ ) impedances of the line. Both  $Z_{1L}$  and  $Z_{0L}$  are needed when calculating the zero-sequence current compensation factor ( $k_0$ ) shown in (1). The  $k_0$  is a setting that is a function of the  $Z_{1L}$  and  $Z_{0L}$  of a line and used in the calculation for a phase-to-ground fault.

$$k_0 = \frac{Z_{0L} - Z_{1L}}{3 \cdot Z_{1L}} \quad (1)$$

For a phase-to-ground fault, distance elements operate when the apparent impedance ( $Z_{APP}$ ) seen by the relay becomes less than the zone reach setting. The apparent impedance is calculated using (2)—a combination of the  $k_0$  setting, measured zero-sequence current ( $I_0$ ), and measured voltage and current of the faulted phase ( $V_\phi$  and  $I_\phi$ , where  $\phi = A, B, \text{ or } C$ ).

$$Z_\phi = \frac{V_\phi}{I_\phi + k_0 \cdot (3 \cdot I_0)} \quad (2)$$

In addition to their use with distance elements, line impedances are used in calculating forward and reverse thresholds for impedance-based directional elements. Directional

elements are used in distance relays to decide if the fault is forward or reverse. These elements are also used to supervise distance elements zone reach settings

This research proposes a method to measure transmission line parameters for protective relay settings. These parameters are both the positive- and zero-sequence impedance of the transmission line. For parallel transmission lines, in addition to the positive- and zero-sequence impedance of the line, the zero-sequence mutual coupling will be measured as well. This method relies on synchronized phasor measurements taken at both ends of the line and compares them with the calculations from both the equivalent PI circuit and the distributed constant line parameters. This comparison determines which method provides more accuracy for determining relay settings. The method used for the calculation depends on whether the line is transposed or untransposed. The performance of the proposed method is verified using PSCAD<sup>TM</sup>/EMTDC<sup>TM</sup> simulation software, filed data from Entergy PMUs installed on a transmission line, and digital real-time simulation.

The contribution of this research is to provide a method to verify in-service transmission line distance relay settings using measurements from PMUs. The measurements are used to calculate transmission line and distance relay settings parameters for both transposed and untransposed lines and compare them to existing settings. This comparison validates relay settings or provides feedback for improvement in the case of discrepancies.

Prior to presenting and analyzing the results, a theoretical review of transmission line parameters theory and equations developed are presented in Chapter 2. Also, Chapter 2 presents a brief overview of synchrophasors technology and the proposed solution methods for calculating the admittance and impedance matrices. Chapter 3 is a paper that was previously



presented at the Georgia Tech Power Systems Conference and the Western Protective Relay Conference (WPRC), showing the proposed method and results for a single transmission line case. It also includes field data from live synchronized phasor measurements installed at a utility transmission line and compares the calculation from the measured data with actual relay settings. It also proposes a method for validating the relay settings. Chapter 4 discusses the RTDS set up and results. Chapter 5 extends the method to parallel transmission lines and provides a method for estimating the zero-sequence mutual coupling in addition to the positive- and zero-sequence impedance of the transmission line. Chapter 6 includes the conclusion and future work.

## Chapter 1 Review of Key Concepts and Literature

### 1.1 Software Tools

Many companies use computer software packages to model their transmission lines and calculate line impedance values. ASPEN Line Constants Program<sup>™</sup>, Electrocon Computer-Aided Protection Engineering (CAPE), Transmission Line Constant Calculation, and EMTDC/PSCAD LCC module are among several software packages that can perform these functions. The software allows the user to model both the physical configuration of the conductors as well as the electrical characteristics of the line. The parameters that the software requires include the number of phase and ground conductors, the conductor type, how far apart each conductor is from the ground and from other conductors, any bundling of conductors, ground resistivity, and so on. Software packages also allow the user to account for conductor sag, and they normally include a database that has diameter, ac resistance, and reactance information for common conductor types. Figure 1 and Figure 2 shows an example of a circuit in a single right of way modeled in the ASPEN Line Constants Program.

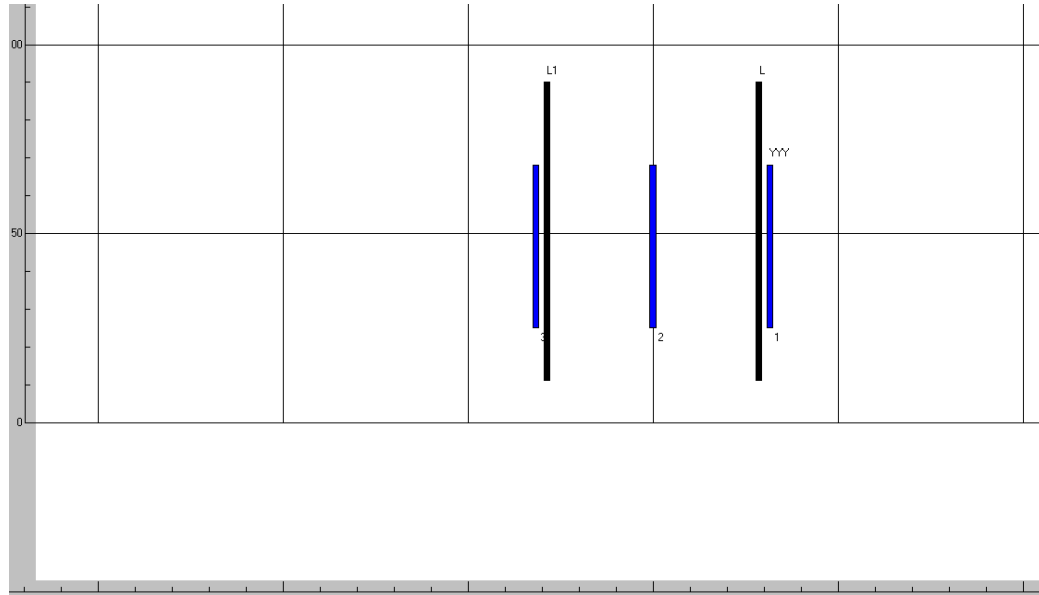


**Figure 1 Aspen Model of a Transmission Line Showing Three Phases and Two Ground Wires**

**Figure 2 ASPEN Line Constants Program Screen Captures Showing the Physical Configuration of a Transmission Line**

The software also allows the user to split an entire right of way into different sections, each with a different physical construction. This allows for instances when one circuit might be parallel to another down a right of way, but only for a certain distance.

Reports from these software tools give line impedance values that can be used in load flow studies, short-circuit and relay coordination studies, and relay settings. It is important that the information entered in the software for the line models is as accurate as possible.

## **1.2 Impedance Measurements Using Test Equipment**

Another way to determine or validate line impedance is by using a test set. One test set that is currently available from Omicron allows for the measurement of ground resistivity and line impedances (with or without mutual coupling of parallel lines). Ground resistivity is measured with the test set as a standalone unit using a four-point test, as described in [12]. Line impedance testing is performed with the test set in conjunction with a coupling unit that injects currents into the de-energized test line and sends voltage measurements back to the test set. One unique characteristic of this unit is its ability to produce test signals that differ from the system frequency. Test current frequencies may range from 15 to 400 Hz, but testing is often performed at 40 Hz, 80 Hz, and a few higher frequencies that are selected by the user in order to reduce interference from other electrical sources. When mutual coupling from parallel lines is not present, the impedance tests are performed seven times to measure different loop combinations—each single-phase-to-ground loop (3 times), each phase-to-phase loop (3 times), and a three-phase-to-ground loop (1 time)—with all three phases grounded at the remote end during each test. Current is injected and voltage is measured for each test as shown in Figure 3. After the tests for all seven loop combinations are performed, the test set uses the measured voltages and injected currents to calculate the line impedance by processing the combined results from all tests through an algorithm.

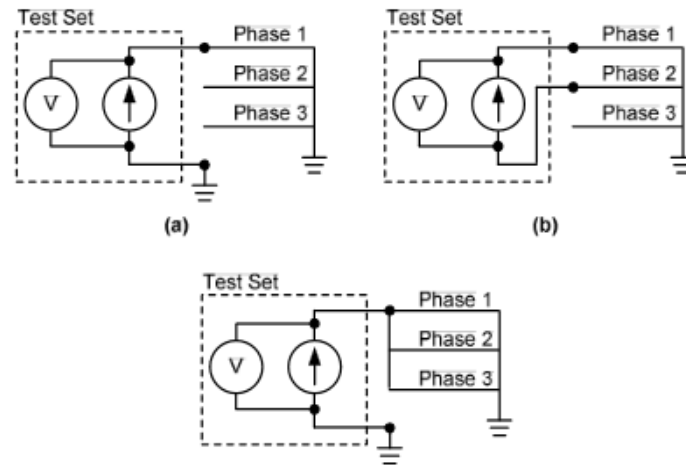


**Figure 3 Test Set Connections for a (a) Single-Phase-to-Ground Loop Test, (b) Phase-to-Phase Loop Test, and (c) Three-Phase-to-Ground Loop Test**

If mutual coupling from parallel lines is present on the test line, the same seven tests are performed three times with 1) the parallel line energized, 2) the parallel line de-energized, floating on one end and grounded at the other, and 3) the parallel line de-energized and grounded at both ends. This makes a total of 21 tests.

### 1.3 Methods for the Calculation of Transmission Line Impedance

Reference [1] focuses on short transmission lines to compute the positive-sequence line impedance using positive-sequence current and voltage. This reference compares four methods that can be employed to estimate the transmission line impedance parameters: Single measurement method, double measurement method, multiple measurement method using linear regression and multiple measurement method using non-linear regression. Among the four methods presented, the multiple measurement method using linear regression was found to be superior. It also found acceptable performance when calculating the series reactance and shunt susceptance when random noise and bias error is present in the measurement. The series resistance calculated was still very sensitive to random noise. This error will affect the

positive-sequence angle measured. This reference acknowledges the limitation of this method for untransposed lines to calculate the positive-sequence impedance.

Reference [2] presents an adaptive transmission line protection scheme based on synchronized phasor measurements. The impedance and admittance matrices calculated for this scheme use only positive-sequence voltage and current. It also measures zero-sequence and negative-sequence quantities when needed. It is not clear if the line that this scheme was tested on is transposed or untransposed.

Reference [3] proposes an offline total least squares method to estimate the positive-sequence line parameters of a transmission line using phasor measurements. It also presents a data selection method for the estimation process to eliminate redundancy in the phasor information and to give variability in the phasor data for better estimation results.

For fully transposed transmission lines, the three sequence networks (positive, negative, and zero) are completely decoupled and the positive-sequence impedance parameters are determined by only the positive-sequence voltages and currents. However, for untransposed transmission lines or transmission lines that are not fully transposed, the three sequence networks are mutually coupled. Using only the positive-sequence measurements to estimate the positive-sequence parameters in these cases can generate inaccurate parameter estimates.

Reference [4] addresses zero-sequence parameters and describes the requirements for introducing an unbalance by tripping and reclosing a single-phase circuit breaker automatically or with an external voltage source. This live line measurement method is based on differential equations algorithm and can measure both the zero-sequence self-impedance and mutual impedance of transmission lines. A feature of this method the author's state is that

it can be used on a live line and measure the zero-sequence parameters of transmission lines, while the conventional measurement method can only be used under the condition that all the transmission lines with mutual inductances must be withdrawn from normal operation. This method also assumes that the line is transposed, and it did not address untransposed lines.

References [1] through [4] provide theoretical and simulation analysis, but they do not show practical implementation or a comparison of the results with data from field-installed synchrophasor units.

#### 1.4 Relay Settings Overview

Figure 4 shows a double-ended line with distance relays at each end of the line. Once the positive-sequence and zero-sequence impedances of the line are determined. These values will be used in the relay settings, as well as for the calculation of zone reach settings as described in this section.

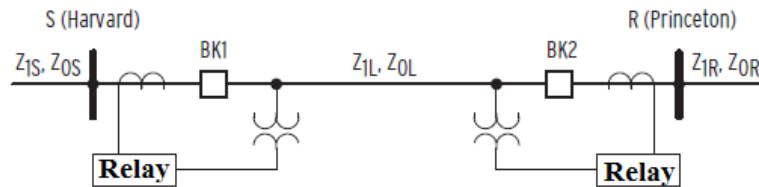


**Figure 4 Overhead Transmission Line With Protection at Each End**

The values of the positive- and zero-sequence impedances are converted from primary to secondary values. The impedances are converted to secondary ohms as follows:

$$k = \frac{CTR}{PTR} \quad (3)$$

and

$$Z_{lsec} = k \cdot Z_{lprimary} \quad (4)$$

The line parameters are entered as shown in Figure 5.

Z1MAG Positive-Sequence Line Impedance Magnitude (ohms,sec)  
7.80 Range = 0.05 to 255.00

Z1ANG Positive-Sequence Line Impedance Angle (deg)  
84.00 Range = 5.00 to 90.00

Z0MAG Zero-Sequence Line Impedance Magnitude (ohms,sec)  
24.80 Range = 0.05 to 255.00

Z0ANG Zero-Sequence Line Impedance Angle (deg)  
81.50 Range = 5.00 to 90.00

EFLOC Fault Location  
Y Select: Y, N

LL Line Length  
100.00 Range = 0.10 to 999.00

**Figure 5 Relay Settings for Transmission Line Parameters**

#### 1.4.1 Zone Distance Settings

##### 1.4.1.1 Zone 1 Phase Distance Element Reach

Zone 1 phase distance protection provides instantaneous protection for phase-to-phase, phase-to phase-to-ground, and three-phase faults in the first 80 percent of the transmission line.

Errors in the current transformers (CTs) and potential transformers (PTs), modeled transmission line data, and fault study data do not permit setting Zone 1 for 100 percent of the transmission line. If Zone 1 is set for 100 percent of the transmission line, unwanted tripping could occur for faults just beyond the remote end of the line.[16]

$$Z1MP = 0.8 \cdot Z1L \quad (5)$$

##### 1.4.1.2 Zone 2 Phase Distance Element Reach

Zone 2 phase distance protection must have adequate reach to detect all phase-to-phase, phase-to phase-to-ground, and three-phase faults along the protected line to make certain that



delayed tripping occurs for faults located in the last 20 percent of the line. Set Zone 2 phase distance reach equal to 120 percent of the positive-sequence impedance of the transmission line.

$$Z2MP = 1.2 \cdot Z1L \quad (6)$$

#### 1.4.1.3 Zone 3 Phase Distance Element Reach

Zone 3 forward phase distance protection is set as backup with a time delay to cover the next adjacent longest line. Coordination study and load analysis must be performed to ensure correct settings.

#### 1.4.2 Ground Distance Elements

Both Zone 1 and Zone 2 ground distance elements must meet the same requirement as for Zone 1 mho phase distance protection.

Z1MP	Zone 1 Reach (ohms,sec)	<input type="text" value="6.24"/>	Range = 0.05 to 64.00, OFF
Z2MP	Zone 2 Reach (ohms,sec)	<input type="text" value="9.36"/>	Range = 0.05 to 64.00, OFF
Z3MP	Zone 3 Reach (ohms,sec)	<input type="text" value="1.87"/>	Range = 0.05 to 64.00, OFF
Z4MP	Zone 4 Reach (ohms,sec)	<input type="text" value="OFF"/>	Range = 0.05 to 64.00, OFF
Z5MP	Zone 5 Reach (ohms,sec)	<input type="text" value="OFF"/>	Range = 0.05 to 64.00, OFF

**Figure 6 Relay Settings for Mho Phase Distance Protection**

Z1MG Zone 1 (ohms,sec)	<input type="text" value="6.24"/>	Range = 0.05 to 64.00, OFF
Z2MG Zone 2 (ohms,sec)	<input type="text" value="9.36"/>	Range = 0.05 to 64.00, OFF
Z3MG Zone 3 (ohms,sec)	<input type="text" value="1.87"/>	Range = 0.05 to 64.00, OFF
Z4MG Zone 4 (ohms,sec)	<input type="text" value="OFF"/>	Range = 0.05 to 64.00, OFF
Z5MG Zone 5 (ohms,sec)	<input type="text" value="OFF"/>	Range = 0.05 to 64.00, OFF

**Figure 7 Relay Settings for Mho Ground Distance Protection**

### 1.4.3 Zero-Sequence Compensation Factor

Zero-sequence current compensation helps to keep the phase and ground distance elements at the same reach if the reach is set equal per zone (e.g.,  $Z1MP = Z1MG$ ). Ground distance elements should measure fault impedance in terms of positive-sequence impedance only.

The calculation for the zero-sequence compensation factor is defined in (1).

k0M1 Zone 1 ZSC Factor Magnitude	<input type="text" value="0.726"/>	Range = 0.000 to 10.000, AUTO
k0A1 Zone 1 ZSC Factor Angle (deg)	<input type="text" value="-3.69"/>	Range = -179.99 to 180.00

**Figure 8 Relay Settings for Zero-Sequence Compensation Factor**

Other settings that rely on the line impedance are directional elements. These parameters calculate the forward and reverse threshold based on the transmission line impedance.

## Chapter 2 Transmission Line Theory and Modeling

### 2.1 Overview of the Transmission Line Parameter Calculation

Transmission lines are one of the major components of an electric power system. Electric power is transferred from generating stations to load centers, usually separated by long distances through transmission lines. The design of a transmission line depends on four electrical parameters:

- Series resistance
- Series inductance
- Shunt capacitance
- Shunt conductance

The series resistance relies basically on the physical composition of the conductor at a given temperature. The series inductance and shunt capacitance are produced by the presence of magnetic and electric fields around the conductors and depend on their geometrical arrangement. The shunt conductance is due to leakage currents flowing across insulators and air. Because leakage current is considerably small compared to nominal current, it is usually neglected, and therefore, shunt conductance is normally not considered for the transmission line modeling.

The following is the calculation of these parameters for three-phase transmission line.

#### 2.1.1 Transmission Line Series Impedance

When the analysis of two conductors carrying currents in a parallel path, as shown in Figure 9(a), is performed using basic electromagnetic flux linkage equations [7], the following equations define the self and mutual impedances:

$$Z_{aa} = r_a + j\omega * \frac{\mu_0}{2\pi} \left(\frac{f}{60}\right) \ln\left(\frac{1}{GMR_a}\right) \text{ ohms/m} \tag{7}$$

$$Z_{ab} = j\omega * \frac{\mu_0}{2\pi} \left(\frac{f}{60}\right) \ln\left(\frac{1}{d_{ab}}\right) \text{ ohms/m} \tag{8}$$

$$\mu_0 = 4\pi * 10^{-7}$$

Equations (7) and (8) are valid for two conductors in free space, running in parallel with a distance,  $d_{ab}$ , between them. The term  $r_a$  is the resistance of the conductor, and GMR is its geometric mean radius.

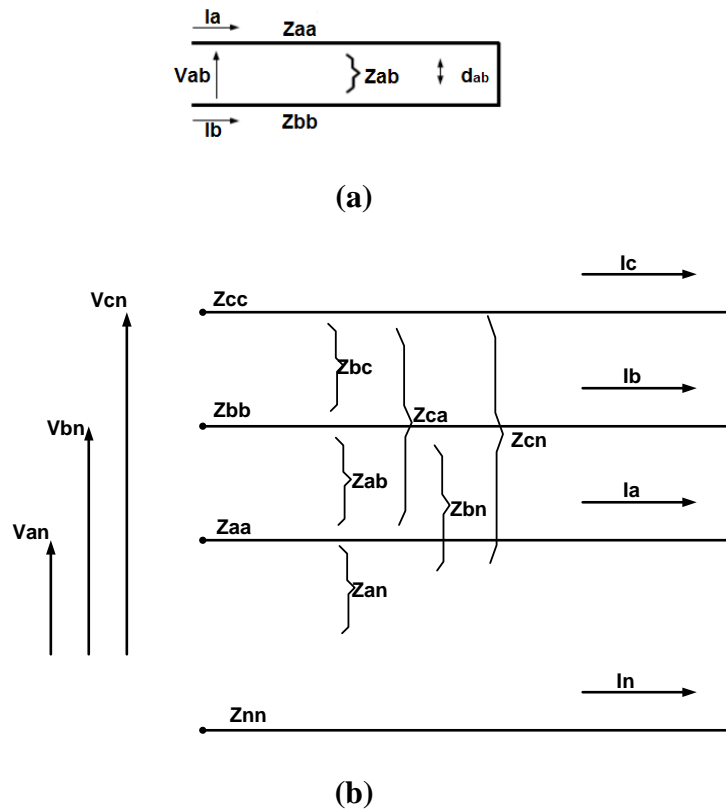


**Figure 9 (a) Two-Conductor Model (b) Three-Phase System With Ground Conductor**

In a three-phase power system, the ground return could be modeled with an equivalent ground conductor, as shown in Figure 9(b). The matrix in (9) is used to relate the voltage drop from one end of each line to the other end of the line in terms of line and neutral currents [7].

$$\begin{bmatrix} V_a \\ V_b \\ V_c \\ V_n \end{bmatrix} \begin{bmatrix} Z_{aa} & Z_{ab} & Z_{ac} & Z_{an} \\ Z_{ba} & Z_{bb} & Z_{bc} & Z_{bn} \\ Z_{ca} & Z_{cb} & Z_{cc} & Z_{cn} \\ Z_{na} & Z_{nb} & Z_{nc} & Z_{nn} \end{bmatrix} \cdot \begin{bmatrix} I_a \\ I_b \\ I_c \\ I_n \end{bmatrix} \quad (9)$$

To simplify (9) and completely eliminate the influence of the neutral current  $I_n$  from the analysis and reduce (9) to a 3 row equation matrix that calculates only A, B and C quantities. The method used is a Kron Reduction, described in detail in [22].

The equation simplifies to:

$$\begin{bmatrix} V_a \\ V_b \\ V_c \end{bmatrix} \begin{bmatrix} Z_{AA} & Z_{AB} & Z_{CA} \\ Z_{AB} & Z_{BB} & Z_{BC} \\ Z_{CA} & Z_{BC} & Z_{CC} \end{bmatrix} \cdot \begin{bmatrix} I_a \\ I_b \\ I_c \end{bmatrix} \quad (10)$$

Where  $Z_{AA}$  is the self-impedance of the “a” conductor, and the  $Z_{AB}$  and  $Z_{CA}$  impedances are the mutual impedances to the “b” and “c” conductors, respectively.

Using (7) and (8) to find the expressions for  $Z_{AA}$ ,  $Z_{AB}$ , and  $Z_{CA}$  and further mathematical simplifications, the impedances are defined by the following equations [11]:

$$Z_{AA} = r_a + r_n + j\omega * \frac{\mu_0}{2\pi} \left(\frac{f}{60}\right) \left[ \ln\left(\frac{1}{GMR_a}\right) + \ln\left(\frac{dan^2}{GMR_n}\right) \right] \text{ ohms/m} \quad (11)$$

$$Z_{AB} = r_n + j\omega * \frac{\mu_0}{2\pi} \left(\frac{f}{60}\right) \left[ \ln\left(\frac{1}{d_{ab}}\right) + \ln\left(\frac{dan \cdot dbn}{GMR_n}\right) \right] \text{ ohms/m} \quad (12)$$

$$ZCA = j\omega * \frac{\mu_0}{2\pi} \left(\frac{f}{60}\right) \left[ \ln\left(\frac{1}{dca}\right) + \ln\left(\frac{dcn \ dan}{GMRn}\right) \right] \text{ ohms/m} \quad (13)$$

Equations (11), (12), and (13) are valid for the phase “a” conductor, where  $r_a$  is the resistance of the “a” conductor;  $r_n$  is the resistance of the return conductor;  $GMR_a$  and  $GMR_n$  are the geometric mean radius of the “a” and “n” conductors, respectively; and  $d_{ab}$ ,  $d_{ca}$ ,  $d_{an}$ ,  $d_{bn}$ , and  $d_{cn}$  are the distances between the assumed conductors.

The same procedure can be followed for the “b” and “c” conductors, and expressions similar to (11), (12), and (13) can be derived. The above development has effectively removed the ground return from the self and mutual impedances of the three conductors in Figure 9(b).

In 1926, John Carson published a classic paper deriving equations for electromagnetic waves propagating in electrical conductors and returning through ground [14]. While the mathematics remains complex and an obscure subject to many, the results can be equated to the previous analysis.

There are other variations of equations to calculate ground current path impedances, such as a concept that uses impedances based on a complex number for the depth of an equivalent underground conductor. These assumptions in the calculation of ground current path can yield errors in the calculation of the zero-sequence impedance.

Another unknown factor that has big impact on the calculation of the zero-sequence impedance is the ground resistivity; the soil material and its physical conditions, like moisture content and temperature. For example, soil with quartz grains have a thermal resistivity of  $11^\circ\text{C-cm/W}$ , water is 165, organic can be from 400 wet to 700 dry, and air is 4,000. Thus, it is generally concluded that soil with the lowest thermal resistivity has a maximum amount of

soil grains and water while having a minimum amount of air. Simply stated, the resistivity of sandy dry soil, such as in Nevada, will be very different from the silty-clay-organic soil in Illinois. Also, river bottom soil will be vastly different than the soil on top of a ridge or bluff within the same general area.

Resistivity is measured in ohm-cm. Variations in soil compositions are as vast as the ranges of published soil resistivity [13]. Generally, clay-silty-loam soils have much lower values (e.g., 4,000 ohm-cm average per one data source) than sandy soils (e.g., 94,000 ohm-cm average per the same data source) [13]. The very nature of the soil and the factors that determine resistivity equate to a dynamically changing value of resistivity. The transmission line in Nevada will have a different local resistivity during a major precipitation event than during a drought.

To emphasize the affect that resistivity can have on a given line, [23] shows the effect of ground resistivity on the zero-sequence impedance of a typical 400 kV line and is show in Figure 10.

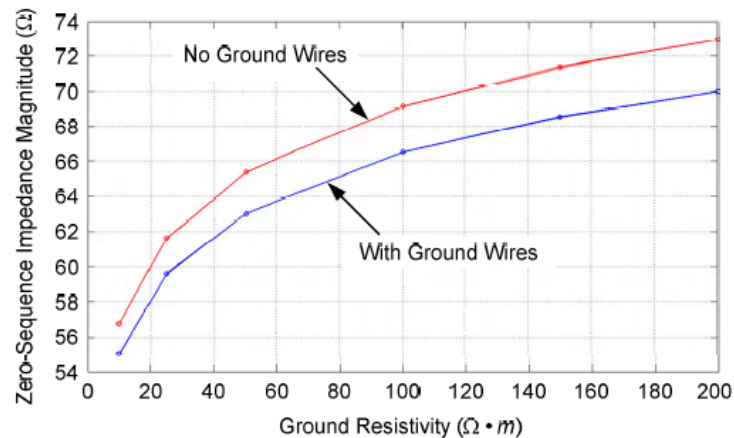


**Figure 10 Effect of Ground Resistivity on Zero-Sequence Impedance Magnitude**

The important point to the protection engineer is that the physical characteristics of a transmission line must be known to accurately model it, resistivity notwithstanding. If certain factors are not addressed the model will be inaccurate. For example, the season of the year, like when the soil is saturated, or if a company that encompasses different geological areas uses a “standard” resistivity value, the model accuracy can be compromised.

Carson’s results are equations that use hyperbolic functions, and approximations can be made for power system frequencies [11] using equivalent mathematical series for these hyperbolic functions [5] [22]. Equations (14) and (15) are the resulting modified Carson equations for self and mutual impedances for any “i” and “j” conductors above ground with a typical earth resistivity of 100 ohms/m<sup>3</sup>.

$$Z_{ii} = r_i + 0.05919 \left( \frac{f}{60} \right) + j0.07537 \left( \frac{f}{60} \right) \left[ \ln \left( \frac{1}{\text{GMR}_i} \right) + 6.74580 \right] \text{ohms / km} \quad (14)$$

$$Z_{ij} = 0.05919 \left( \frac{f}{60} \right) + j0.07537 \left( \frac{f}{60} \right) \left[ \ln \left( \frac{1}{d_{ij}} \right) + 6.74580 \right] \text{ohms / km} \quad (15)$$

Equations (14) and (15) are similar to (11) and (12). They have the same form and can be used to calculate the self and mutual impedances of any arrangement of conductors above ground.

For any arrangement of conductors (a, b, and c) of a single-circuit transmission line, the matrix  $Z$  describes the line impedances using (14) and (15):

$$Z = \begin{bmatrix} Z_{aa} & Z_{ab} & Z_{ac} \\ Z_{ab} & Z_{bb} & Z_{bc} \\ Z_{ac} & Z_{bc} & Z_{cc} \end{bmatrix} \quad (16)$$



Equation (16) is referred to as the phase impedance matrix. When ground wires are present, they can be included in the above matrices using Kron's reduction technique. When bundled conductors are used in the transmission line phases, the impedance matrix becomes quite large. With proper matrix reduction techniques, an equivalent impedance matrix can also be obtained.

### 2.1.2 Transmission Line Shunt Admittance Matrix

Capacitance exists among transmission line conductors due to their potential difference.

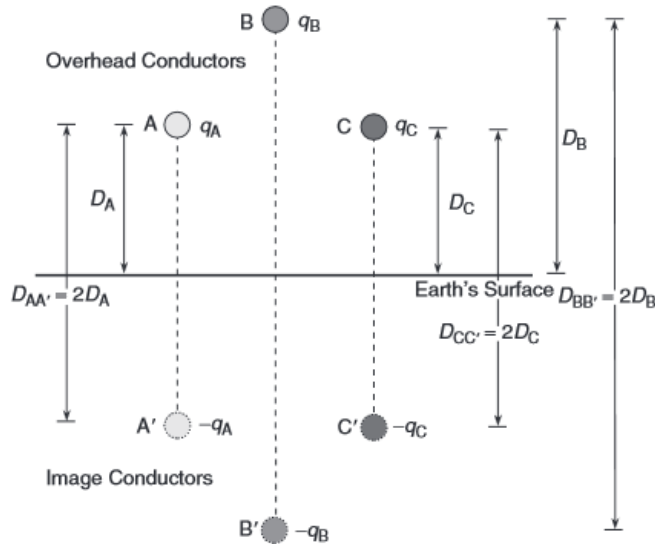


**Figure 11 Arrangements of Image Conductors in a Three-Phase Transmission Line**

The potential coefficient matrix P is defined as:

$$P = \frac{1}{2\pi\epsilon_0} \begin{bmatrix} \ln\left(\frac{H_{aai}}{r}\right) & \ln\left(\frac{H_{abi}}{D_{ab}}\right) & \ln\left(\frac{H_{aci}}{D_{ac}}\right) \\ \ln\left(\frac{H_{abi}}{D_{ab}}\right) & \ln\left(\frac{H_{bbi}}{r}\right) & \ln\left(\frac{H_{bci}}{D_{bc}}\right) \\ \ln\left(\frac{H_{aci}}{D_{ac}}\right) & \ln\left(\frac{H_{bci}}{D_{bc}}\right) & \ln\left(\frac{H_{cc i}}{r}\right) \end{bmatrix} \quad (17)$$

And the admittance matrix is found using (18).

$$Y = j \cdot \omega \cdot P^{-1} \quad (18)$$

$$Y = \begin{bmatrix} Y_{aa} & Y_{ab} & Y_{ac} \\ Y_{ab} & Y_{bb} & Y_{bc} \\ Y_{ac} & Y_{bc} & Y_{cc} \end{bmatrix} \quad (19)$$

Equation (18) and (19) are the series impedance matrix and admittance matrix that we are solving for.

In actual transmission lines, the phase conductors cannot maintain symmetrical arrangement along the whole length because of construction considerations, even when bundle conductor spacers are used. With asymmetrical spacing, the inductance will be different for each phase, with a corresponding unbalanced voltage drop on each conductor. Therefore, the single-phase equivalent circuit to represent the power system cannot be used.

In a transposed system, each phase conductor occupies the location of the other two phases for one-third of the total line length, as shown in Figure 12. In this case, the average distance geometrical mean distance (GMD) substitutes distance,  $D$ , and the calculation of phase inductance derived for symmetrical arrangement is still valid.

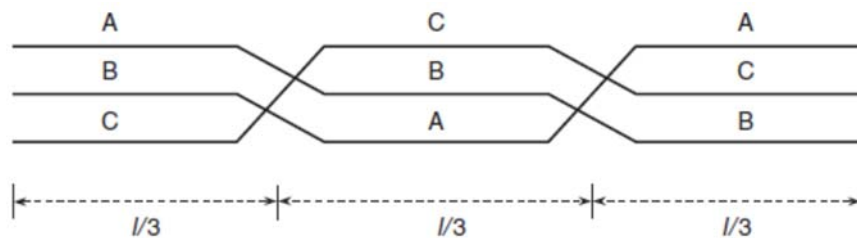


**Figure 12 Transposed Transmission Line**

The impedance matrix reduces to:

$$Z = \begin{bmatrix} Z_{\text{self}} & Z_{\text{mutual}} & Z_{\text{mutual}} \\ Z_{\text{mutual}} & Z_{\text{mutual}} & Z_{\text{mutual}} \\ Z_{\text{mutual}} & Z_{\text{mutual}} & Z_{\text{self}} \end{bmatrix} \quad (20)$$

And the admittance matrix to:

$$Y = \begin{bmatrix} Y_{\text{self}} & Y_{\text{mutual}} & Y_{\text{mutual}} \\ Y_{\text{mutual}} & Y_{\text{mutual}} & Y_{\text{mutual}} \\ Y_{\text{mutual}} & Y_{\text{mutual}} & Y_{\text{self}} \end{bmatrix} \quad (21)$$

Equations (20) and (21) are the self-impedance and admittance matrices, respectively, that we are solving for in the case of transposed transmission lines. The number of unknowns in these matrices for the case of transposed lines is reduced compared to the matrices for lines that are untransposed. This makes the solution and conditions to solve for each case different, as will be shown in Chapter 3.

## 2.2 Transmission Line Modeling

The line parameters described in the previous section are used to model the transmission line and perform calculations. The arrangement of the parameters (equivalent circuit model) representing the line depends on the length of the line.

A transmission line is defined as a short-length line if its length is less than 80 km (50 miles). In this case, the shunt capacitance effect is negligible and only the resistance and inductive reactance are considered. Assuming balanced conditions, the line can be represented by the equivalent circuit of a single phase with resistance,  $R$ , and inductive reactance,  $X_L$ , in series (series impedance). If the transmission line has a length between 80 km (50 miles) and 240

km (150 miles), the line is considered a medium-length line and its single-phase equivalent circuit can be represented in a nominal  $\pi$  circuit configuration [18]. The shunt capacitance of the line is divided into two equal parts, each placed at the sending and receiving ends of the line. Figure 13 shows the equivalent circuit for a medium-length line.

Both short- and medium-length transmission lines use approximated lumped-parameter models. However, if the line is larger than 240 km, the model must consider parameters uniformly distributed along the line. The appropriate series impedance and shunt capacitance are found by solving the corresponding differential equations, where voltages and currents are described as a function of distance and time. Figure 14 shows the equivalent circuit for a long line.

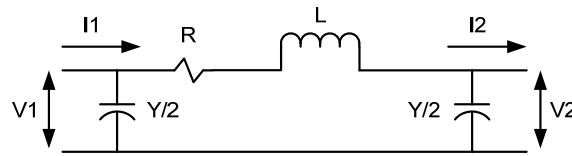


**Figure 13** Equivalent PI Circuit of a Three-Phase Transmission line

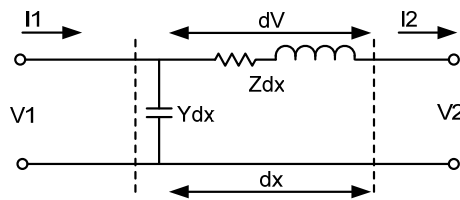


**Figure 14** Distributed Parameter Circuit of a Transmission line

The voltages and currents are  $3 \times 1$  complex vectors of the form:

$$V1 = \begin{bmatrix} V1A \\ V1B \\ V1C \end{bmatrix} \quad I1 = \begin{bmatrix} I1A \\ I1B \\ I1C \end{bmatrix} \quad V2 = \begin{bmatrix} V2A \\ V2B \\ V2C \end{bmatrix} \quad I2 = \begin{bmatrix} I2A \\ I2B \\ I2C \end{bmatrix} \quad (22)$$

These quantities will be measured via synchrophasors for each line the validation of the relay settings is to be implemented. The solution is developed first for the calculation of the  $Y$  admittance and  $Z$  impedance matrices. Then a symmetrical transformation is used on these matrices to extract the positive- and zero-sequence of the transmission line.

Next, an overview of the synchrophasor technology will be presented.

### **2.3 Synchrophasors Overview**

The word synchrophasor is derived from two words: synchronized phasor. Synchrophasor measurement refers to the concept of providing measurements taken on a synchronized schedule in multiple locations. A high-accuracy clock, commonly a Global Positioning System (GPS) receiver, makes synchrophasor measurement possible [26] [27].

Synchronized phasor measurements, or synchrophasors, provide a method for comparing phase and sequence values from anywhere on a power system [24]. The method of collecting and using this information impacts communications and data processing requirements. These requirements can vary from a serial cable and hand-held calculator to a 1 Gbps Ethernet network with multitiered data concentrators and server synchrophasors and provide a means for comparing a phasor to an absolute time reference. This is similar to putting a timing mark on a virtual generator shaft anywhere on the system and connecting a strobe light source to a single reference point for the entire system. The availability of high-accuracy satellite-synchronized clocks makes synchronized phasor measurement possible. Through the use of the clock, the phasor measurement unit (PMU) produces a reference sinusoidal wave. This reference wave is a nominal frequency sinusoidal wave for which maximum occurs at the

exact start of each second. The measured local voltage or current is then compared to this reference wave, as shown in Figure 15 below.

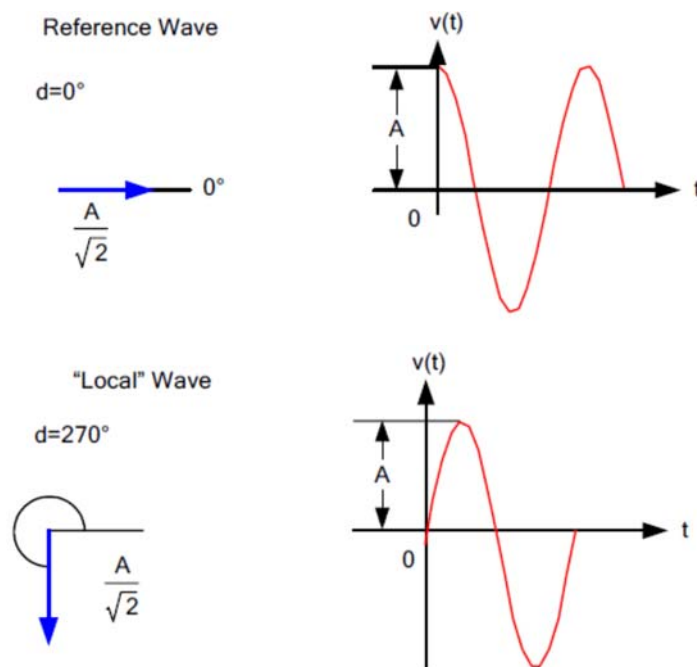


**Figure 15 Reference Wave and “Local” Wave With Angular Comparison**

Because the reference wave is only dependent on a GPS-generated time signal, this wave will be the same at all different PMU locations. Therefore, a local phasor can be compared with a phasor at any other location, and the angular difference between the two phasors represents the absolute difference between the two locations.

## 2.4 Transposed Lines

### 2.4.1 Equivalent Pi Solution Algorithm

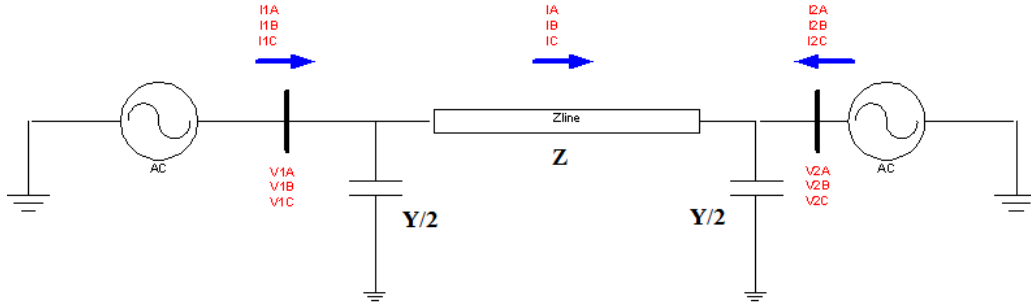


**Figure 16 Equivalent Pi Diagram Showing Current Voltages and the Unknown Parameters  $Z$  and  $Y$**

If we define:

$$I_A = I_{1A} + I_{2A} \quad I_B = I_{1B} + I_{2B} \quad I_C = I_{1C} + I_{2C} \quad (23)$$

$$V_A = V_{1A} + V_{2A} \quad V_B = V_{1B} + V_{2B} \quad V_C = V_{1C} + V_{2C} \quad (24)$$

Below is the development of the solution for the  $Y$  admittance matrix.

The current as a function of the  $Y$  admittance is:

$$\begin{bmatrix} I_A \\ I_B \\ I_C \end{bmatrix} = \begin{bmatrix} Y_1 & Y_2 & Y_3 \\ Y_2 & Y_1 & Y_2 \\ Y_3 & Y_2 & Y_1 \end{bmatrix} \cdot \begin{bmatrix} V_A \\ V_B \\ V_C \end{bmatrix} \quad (25)$$

Rearranging to solve for the  $Y$  parameters:

$$\begin{bmatrix} I_A \\ I_B \\ I_C \end{bmatrix} = \begin{bmatrix} V_A & V_B & V_C \\ V_B & V_A + V_C & 0 \\ V_C & V_B & V_A \end{bmatrix} \cdot \begin{bmatrix} Y_1 \\ Y_2 \\ Y_3 \end{bmatrix} \quad (26)$$

$$\begin{bmatrix} Y1 \\ Y2 \\ Y3 \end{bmatrix} = \begin{bmatrix} VA & VB & VC \\ VB & VA+VC & 0 \\ VC & VB & VA \end{bmatrix}^{-1} \cdot \begin{bmatrix} IA \\ IB \\ IC \end{bmatrix} \quad (27)$$

Below is the development of the solution for the Z impedance matrix.

If we define the line current:

$$\begin{bmatrix} ILA \\ ILB \\ ILC \end{bmatrix} = \begin{bmatrix} IIA \\ IIB \\ IIC \end{bmatrix} - \begin{bmatrix} Y1 & Y2 & Y3 \\ Y2 & Y1 & Y2 \\ Y3 & Y2 & Y1 \end{bmatrix} \cdot \begin{bmatrix} V1A \\ V1B \\ V1C \end{bmatrix} \quad (28)$$

And define the voltage across the series impedance:

$$VZA = V1A - V2A \quad VZB = V1B - V2B \quad VZC = V1C - V2C \quad (29)$$

Then, the voltage as a function of the series impedance Z:

$$\begin{bmatrix} VZA \\ VZB \\ VZC \end{bmatrix} = \begin{bmatrix} Z1 & Z2 & Z3 \\ Z2 & Z1 & Z2 \\ Z3 & Z2 & Z1 \end{bmatrix} \cdot \begin{bmatrix} ILA \\ ILB \\ ILC \end{bmatrix} \quad (30)$$

Rearranging to solve for the Z parameters:

$$\begin{bmatrix} VZA \\ VZB \\ VZC \end{bmatrix} = \begin{bmatrix} ILA & ILB & ILC \\ ILB & ILA+ILC & 0 \\ ILC & ILB & ILA \end{bmatrix} \cdot \begin{bmatrix} Z1 \\ Z2 \\ Z3 \end{bmatrix} \quad (31)$$

$$\begin{bmatrix} Z1 \\ Z2 \\ Z3 \end{bmatrix} = \begin{bmatrix} ILA & ILB & ILC \\ ILB & ILA+ILC & 0 \\ ILC & ILB & ILA \end{bmatrix}^{-1} \cdot \begin{bmatrix} IA \\ IB \\ IC \end{bmatrix} \quad (32)$$



Once the admittance and series impedance matrices are determined, symmetrical components transformation is applied to obtain the positive- and zero-sequence impedance of the transmission line, as shown below.

$$\begin{aligned} Z_{012} &= A^{-1}.Z.A \\ Y_{012} &= A^{-1}.Y.A \end{aligned} \quad (33)$$

Where:

$$\begin{aligned} a &= 1^{j.120\text{deg}} \\ A &= \begin{bmatrix} 1 & 1 & 1 \\ 1 & a^2 & a \\ 1 & a & a^2 \end{bmatrix} \\ Z &= \begin{bmatrix} Z1 & Z2 & Z3 \\ Z2 & Z1 & Z2 \\ Z3 & Z2 & Z1 \end{bmatrix} \\ Y &= \begin{bmatrix} Y1 & Y2 & Y3 \\ Y2 & Y1 & Y2 \\ Y3 & Y2 & Y1 \end{bmatrix} \end{aligned}$$

The positive- and zero-sequence impedance parameters are extracted from  $Z_{012}$ .

$$Z_{012} = \begin{bmatrix} Z0 & 0 & 0 \\ 0 & Z2 & 0 \\ 0 & 0 & Z1 \end{bmatrix} \quad (34)$$

## 2.4.2 Distributed Parameter Line

### 2.4.2.1 Solution method #1

The differential equations that define the model for the distributed parameter line shown in Figure 14 are (35) and (36).

$$\begin{bmatrix} \frac{dVA(x)}{dx} \\ \frac{dVB(x)}{dx} \\ \frac{dVC(x)}{dx} \end{bmatrix} = \begin{bmatrix} Z1 & Z2 & Z3 \\ Z2 & Z1 & Z2 \\ Z3 & Z2 & Z1 \end{bmatrix} \cdot \begin{bmatrix} IA(x) \\ IB(x) \\ IC(x) \end{bmatrix} \quad (35)$$

$$\begin{bmatrix} \frac{dIA(x)}{dx} \\ \frac{dIB(x)}{dx} \\ \frac{dIC(x)}{dx} \end{bmatrix} = \begin{bmatrix} Y1 & Y2 & Y3 \\ Y2 & Y1 & Y2 \\ Y3 & Y2 & Y1 \end{bmatrix} \cdot \begin{bmatrix} VA(x) \\ VB(x) \\ VC(x) \end{bmatrix} \quad (36)$$

The explicit solution of the differential equations is based on:

$$\begin{bmatrix} V1 \\ I1 \end{bmatrix} = \begin{bmatrix} \cosh(\Gamma l) & \sinh(\Gamma l) Z_0 \\ Y_0 \sinh(\Gamma l) & Y_0 \cosh(\Gamma l) Z_0 \end{bmatrix} \begin{bmatrix} V2 \\ I2 \end{bmatrix} \quad (37)$$

Where:

$$\Gamma = (ZY)^{1/2}$$

$$Z_0 = \Gamma Y^{-1} = \Gamma^{-1} Z$$

$$Y_0 = Y \Gamma^{-1} = Z^{-1} \Gamma$$

The functions to perform the calculations are listed below.

Function to return matrix elements operation:

$$M_f(x, f) := \begin{cases} \text{return } f(x) \text{ if } \text{IsScalar}(x) \\ E \leftarrow \text{eigenvecs}(x) \\ D \leftarrow f(\text{eignevals}(x)) \\ E \cdot \text{diag}(D) \cdot E^{-1} \end{cases} \quad (38)$$

Exponential operation:

$$\text{Exp1}(x) := M_f(x, \text{exp}) \quad (39)$$

Hyperbolic sine function:

$$\text{Sinh}(x) := M_f(x, \text{sinh}) \quad (40)$$

Hyperbolic cosine function:

$$\text{Cosh}(x) := M_f(x, \text{cosh}) \quad (41)$$

Function to return matrix elements square root:

$$\text{SQR}(x) := \begin{cases} E \leftarrow \text{eigenvecs}(x) \\ D \leftarrow \sqrt{\text{eignevals}(x)} \\ E \cdot \text{diag}(D) \cdot E^{-1} \end{cases} \quad (42)$$

$$\text{COSH} := \text{Cosh}(\Gamma)$$

$$\text{SINH} := \text{Sinh}(\Gamma)$$

$$\text{SINZ} := \text{SINH.Zo}$$

$$\text{COSZ} := \text{Yo.COSH.Zo}$$

$$\text{SINY} := \text{Yo.SINH}$$

Then the voltage and currents solution is:

$$\begin{bmatrix} \text{VIA} \\ \text{VIB} \\ \text{VIC} \\ \text{IIA} \\ \text{IIB} \\ \text{IIV} \end{bmatrix} = \begin{bmatrix} \text{COSH}_{0,0} & \text{COSH}_{0,1} & \text{COSH}_{0,2} & \text{SINZ}_{0,0} & \text{SINZ}_{0,1} & \text{SINZ}_{0,2} \\ \text{COSH}_{1,0} & \text{COSH}_{1,1} & \text{COSH}_{1,2} & \text{SINZ}_{1,0} & \text{SINZ}_{1,1} & \text{SINZ}_{1,2} \\ \text{COSH}_{2,0} & \text{COSH}_{2,1} & \text{COSH}_{2,2} & \text{SINZ}_{2,0} & \text{SINZ}_{2,1} & \text{SINZ}_{2,2} \\ \text{SINY}_{0,0} & \text{SINY}_{0,1} & \text{SINY}_{0,2} & \text{COSZ}_{0,0} & \text{COSZ}_{0,1} & \text{COSZ}_{0,2} \\ \text{SINY}_{1,0} & \text{SINY}_{1,1} & \text{SINY}_{1,2} & \text{COSZ}_{1,0} & \text{COSZ}_{1,1} & \text{COSZ}_{1,2} \\ \text{SINY}_{2,0} & \text{SINY}_{2,1} & \text{SINY}_{2,2} & \text{COSZ}_{2,0} & \text{COSZ}_{2,1} & \text{COSZ}_{2,2} \end{bmatrix} \cdot \begin{bmatrix} \text{V2A} \\ \text{V2B} \\ \text{V2C} \\ \text{I2A} \\ \text{I2B} \\ \text{I2B} \end{bmatrix} \quad (43)$$

The voltage and currents are acquired from the synchrophasor measurement. The solution of (43) is using a nonlinear iterative solution using software tools such as Mathcad or Matlab.

#### 2.4.2.2 Solution Method #2

The solution of (35) and (36) is computed using numerical integration in the complex domain [19].

The right-hand side of the ODE system in matrix notation.

Sending end voltage and current matrix:

$$w = \begin{bmatrix} \text{VIA} \\ \text{VIB} \\ \text{VIC} \\ \text{IIA} \\ \text{IIA} \\ \text{IIA} \end{bmatrix} \quad (44)$$

And the matrix of the unknown Y admittance and Z impedance:

$$P = \begin{bmatrix} Z1 \\ Z1 \\ Z1 \\ Y1 \\ Y1 \\ Y1 \end{bmatrix} \quad (45)$$

$$D(x, w, P) = \begin{bmatrix} P_0 & P_1 & P_2 \\ P_1 & P_0 & P_1 \\ P_2 & P_{P1} & P_0 \\ P_3 & P_4 & P_5 \\ P_4 & P_3 & P_4 \\ P_5 & P_4 & P_2 \end{bmatrix} \cdot \begin{bmatrix} -w_3 \\ -w_4 \\ -w_5 \\ -w_0 \\ -w_1 \\ -w_2 \end{bmatrix} \quad (46)$$

Program for numerical integration Euler:

$$\text{Euler(IC, xL, xR, N, D, P)} := \left[ \begin{array}{l} \left[ (Y^{(0)} \leftarrow IC)(X_0 \leftarrow xL) \right] \\ h \leftarrow \frac{(xR - xL)}{N} \\ \text{for } n \in 0..N-1 \\ \left[ (x_L \leftarrow X_n)(y_L \leftarrow Y^{(n)}) \right] \\ x_{mdl} \leftarrow x_L + \frac{h}{2} \\ y_{mdl} \leftarrow y_L + \frac{1}{2} \cdot h \cdot D(x_L, y_L, P) \\ y_R \leftarrow y_L + h \cdot D(x_{mdl}, y_{mdl}, P) \\ \left[ (X_{n+1} \leftarrow x_L + h)(Y^{(n+1)} \leftarrow y_R) \right] \\ \text{augment}(X, Y^T) \end{array} \right] \quad (47)$$

IC is a matrix of the sending end voltage and currents:

$x_L = 0$  starting point

$x_R = 1$  ending point

$N$  = Number of points of integration

The receiving end voltage and current as a function of  $P$  is found using  $XVIP$ , which is a matrix with columns  $x$ ,  $V$ , and  $I$  as integral of ODE.

$$xVIP = \text{Euler}(IC, x_L, x_R, N, D, P) \quad (48)$$

$$\begin{bmatrix} V_{2A} \\ V_{2B} \\ V_{2C} \end{bmatrix} = \begin{bmatrix} xVIP_N^{<1>} \\ xVIP_N^{<2>} \\ xVIP_N^{<3>} \end{bmatrix} \quad (49)$$

$$\begin{bmatrix} I_{2A} \\ I_{2B} \\ I_{2C} \end{bmatrix} = \begin{bmatrix} xVIP_N^{<4>} \\ xVIP_N^{<5>} \\ xVIP_N^{<6>} \end{bmatrix}$$

Matrix  $P$  is found using Mathcad built in iterative nonlinear solver.

## 2.5 Untransposed Transmission Lines

### 2.5.1 Equivalent PI circuit

Matrix  $Y$  and  $Z$  for untransposed lines have 6 unknowns each so the solution to be able to solve the matrices is based on multiple independent states from the power system.

$$\begin{pmatrix} \text{Re}(IA_1) \\ \text{Im}(IA_1) \\ \text{Re}(IB_1) \\ \text{Im}(IB_1) \\ \text{Re}(IC_1) \\ \text{Im}(IC_1) \\ \text{Re}(IA_2) \\ \text{Im}(IA_2) \\ \text{Re}(IB_2) \\ \text{Im}(IB_2) \\ \text{Re}(IC_2) \\ \text{Im}(IC_2) \\ \text{Re}(IA_3) \\ \text{Im}(IA_3) \\ \text{Re}(IB_3) \\ \text{Im}(IB_3) \\ \text{Re}(IC_3) \\ \text{Im}(IC_3) \end{pmatrix} = \begin{pmatrix} -\text{Im}(VA_1) & -\text{Im}(VB_1) & -\text{Im}(VC_1) & 0 & 0 & 0 \\ \text{Re}(VA_1) & \text{Re}(VB_1) & \text{Re}(VC_1) & 0 & 0 & 0 \\ 0 & -\text{Im}(VA_1) & 0 & -\text{Im}(VB_1) & -\text{Im}(VC_1) & 0 \\ 0 & \text{Re}(VA_1) & 0 & \text{Re}(VB_1) & \text{Re}(VC_1) & 0 \\ 0 & 0 & -\text{Im}(VA_1) & 0 & -\text{Im}(VB_1) & -\text{Im}(VC_1) \\ 0 & 0 & \text{Re}(VA_1) & 0 & \text{Re}(VB_1) & \text{Re}(VC_1) \\ -\text{Im}(VA_2) & -\text{Im}(VB_2) & -\text{Im}(VC_2) & 0 & 0 & 0 \\ \text{Re}(VA_2) & \text{Re}(VB_2) & \text{Re}(VC_2) & 0 & 0 & 0 \\ 0 & -\text{Im}(VA_2) & 0 & -\text{Im}(VB_2) & -\text{Im}(VC_2) & 0 \\ 0 & \text{Re}(VA_2) & 0 & \text{Re}(VB_2) & \text{Re}(VC_2) & 0 \\ 0 & 0 & -\text{Im}(VA_2) & 0 & -\text{Im}(VB_2) & -\text{Im}(VC_2) \\ 0 & 0 & \text{Re}(VA_2) & 0 & \text{Re}(VB_2) & \text{Re}(VC_2) \\ -\text{Im}(VA_3) & -\text{Im}(VB_3) & -\text{Im}(VC_3) & 0 & 0 & 0 \\ \text{Re}(VA_3) & \text{Re}(VB_3) & \text{Re}(VC_3) & 0 & 0 & 0 \\ 0 & -\text{Im}(VA_3) & 0 & -\text{Im}(VB_3) & -\text{Im}(VC_3) & 0 \\ 0 & \text{Re}(VA_3) & 0 & \text{Re}(VB_3) & \text{Re}(VC_3) & 0 \\ 0 & 0 & -\text{Im}(VA_3) & 0 & -\text{Im}(VB_3) & -\text{Im}(VC_3) \\ 0 & 0 & \text{Re}(VA_3) & 0 & \text{Re}(VB_3) & \text{Re}(VC_3) \end{pmatrix} \cdot \begin{pmatrix} Y1 \\ Y2 \\ Y3 \\ Y4 \\ Y5 \\ Y6 \end{pmatrix} \quad (50)$$

The subscripts 1, 2, and 3 represent the different states from the power system that are required for the solution. These states represent unbalanced conditions such as remote ground faults in the system.

If the voltage matrix rank is full and the single value decomposition matrix eigenvalues are non-zero, the Y matrix can be solved for using the generalized (pseudo) inverse matrix operation, which gives the least squares solution [8].

Similarly the Z matrix can be solved using the generalized (pseudo) inverse matrix operation, which gives the least squares solution [8].

$$\begin{pmatrix} \text{VZA}_{.1} \\ \text{VZB}_{.1} \\ \text{VZC}_{.1} \\ \text{VZA}_{.2} \\ \text{VZB}_{.2} \\ \text{VZC}_{.2} \\ \text{VZA}_{.3} \\ \text{VZB}_{.3} \\ \text{VZC}_{.3} \end{pmatrix} = \begin{pmatrix} \text{ILA}_{.1} & 0 & 0 & \text{ILB}_{.1} & \text{ILC}_{.1} & 0 \\ 0 & \text{ILB}_{.1} & 0 & \text{ILA}_{.1} & 0 & \text{ILC}_{.1} \\ 0 & 0 & \text{ILC}_{.1} & 0 & \text{ILA}_{.1} & \text{ILB}_{.1} \\ \text{ILA}_{.2} & 0 & 0 & \text{ILB}_{.2} & \text{ILC}_{.2} & 0 \\ 0 & \text{ILB}_{.2} & 0 & \text{ILA}_{.2} & 0 & \text{ILC}_{.2} \\ 0 & 0 & \text{ILC}_{.2} & 0 & \text{ILA}_{.2} & \text{ILB}_{.2} \\ \text{ILA}_{.3} & 0 & 0 & \text{ILB}_{.3} & \text{ILC}_{.3} & 0 \\ 0 & \text{ILB}_{.3} & 0 & \text{ILA}_{.3} & 0 & \text{ILC}_{.3} \\ 0 & 0 & \text{ILC}_{.3} & 0 & \text{ILA}_{.3} & \text{ILB}_{.3} \end{pmatrix} \cdot \begin{pmatrix} \text{Z1} \\ \text{Z2} \\ \text{Z3} \\ \text{Z4} \\ \text{Z5} \\ \text{Z6} \end{pmatrix} \quad (51)$$



## **Chapter 3 Validation of Transmission Line Relay Parameters Using Synchronphasors**

This chapter is a paper that was presented at both the Georgia Tech Relay Conference in April 2014 and the Western Protective Relay Conference (WPRC) in October 2014. The coauthor, Cat Wong, from Entergy transmission provided the synchronphasor field data collected and the relay settings from the existing transmission line used for the case study.

### **3.1 Paper Abstract**

This paper proposes a method to measure transmission line parameters for protective relay settings. This method relies on synchronized phasor measurements taken at both ends of the line and compares them with the calculations from both the equivalent PI circuit and the distributed constant line parameters. This comparison determines which method provides more accuracy for determining relay settings. The method used for the calculation depends on whether the line is transposed or untransposed. The performance of the proposed method is verified using simulation software and field data from Entergy PMUs on a transmission line. This paper discusses the data collected from the PMUs and compares the calculation from the measured data with actual relay settings. Finally, the paper proposes a method for validating the relay settings.

### **3.2 Paper Introduction**

The offline calculation of transmission line impedance has long been used by engineers to determine appropriate distance relay settings. Accurate calculation is paramount for reliable distance relay operation and correct fault location. Transmission line impedance is estimated based on the tower configuration and physical properties of the conductor. These transmission

line impedance estimates are based on assumptions and approximations such as ground resistivity and temperature.

Several methods have previously been proposed to identify transmission line parameters using PMUs. References [1] and [2] use the short-line model for the calculation of only positive-sequence impedance, neglecting the shunt capacitance. Reference [3] includes the shunt capacitance but still only computes the positive-sequence impedance. For fully transposed transmission lines, the three sequence networks (positive, negative, and zero) are completely decoupled and the positive-sequence impedance parameters are determined by only the positive-sequence voltages and currents. However, for untransposed transmission lines or transmission lines that are not fully transposed, the three sequence networks are mutually coupled. Using only the positive-sequence measurements to estimate the positive-sequence parameters in these cases can generate inaccurate parameter estimates.

Reference [4] addresses zero-sequence parameters and describes the requirements for introducing an unbalance by tripping and reclosing a single-phase circuit breaker automatically or with an external voltage source. References [1] through [4] provide theoretical and simulation analysis, but they do not show practical implementation or a comparison of the results with data from field-installed synchrophasor units.

The method proposed in this paper validates the relay settings parameters derived from the positive- and zero-sequence impedances using measurements from synchronized phasors at both ends of a line. The method used for the calculation of the positive- and zero-sequence impedances depends on whether the line is transposed or untransposed. In the case of a transposed line, zero-sequence parameters are calculated from steady-state load conditions if

there is sufficient unbalance in the measured voltage. The minimum amount of unbalance required to perform the calculation is characterized. The equations to calculate the positive- and zero-sequence impedances and shunt admittances for a transposed line can be clearly defined and then solved if there is sufficient standing zero-sequence voltage unbalance during normal system operation. The resulting set of equations is much more difficult to solve using measurements from steady-state operation if the line is untransposed.

In the case of untransposed lines or transposed lines without sufficient measured zero-sequence voltage unbalance, the parameters are calculated based on remote fault conditions involving ground in the system. These fault conditions are not necessarily on the line itself but can be anywhere that can generate enough zero-sequence unbalance. This unbalance is quantified.

In this paper, field data is used from Entergy PMUs installed on a 230 kV transmission line to compare these calculations with the relay settings derived from line constants programs. A method for checking the relay settings is proposed based on the parameter calculations from the PMUs.

This paper is organized as follows:

- Section 3.2 discusses line modeling and the models used for transmission lines.
- Section 3.3 discusses the calculation of parameters for both transposed and untransposed lines. Simulations using PSCAD/EMTDC software are used to validate the results and verify the accuracy and limitations of the calculation method.
- Section 3.4 discusses the setup of synchrophasors on an Entergy line.

- Section 3.5 discusses the results of the parameter calculation and compares them with the line constants and line distance settings that are presently programmed in the relay. A method for validation is then presented.

### 3.3 Line Modeling

Figure 17 shows the model of a three-phase transmission line with mutual impedance [5].

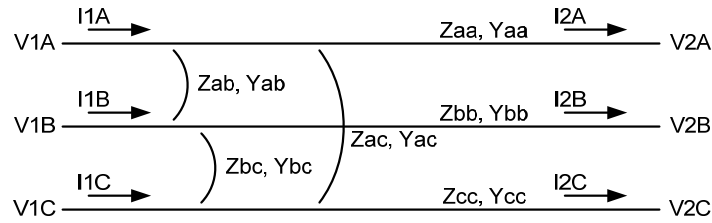


**Figure 17 Model of a Three-Phase Transmission Line With Mutual Impedance**

The transmission line is characterized by four parameters: series resistance  $R$  due to the conductor resistivity, shunt conductance  $G$  due to leakage currents between the phases and ground (this term is neglected because it has a very small impact on the types of studies that use the model), series inductor  $L$  due to the magnetic field surrounding the conductors, and shunt capacitance  $C$  due to the electric field between conductors.

The line parameters are defined by the shunt admittance matrix ( $Y = jB \Omega^{-1}$  per mile) and the series impedance matrix ( $Z = R + jX$  ohms per mile) for a lossless transmission line.

$$Y \begin{bmatrix} Y_{aa} & Y_{ab} & Y_{ac} \\ Y_{ba} & Y_{bb} & Y_{bc} \\ Y_{ca} & Y_{cb} & Y_{cc} \end{bmatrix} \quad (52)$$

$$Z \begin{bmatrix} Z_{aa} & Z_{ab} & Z_{ac} \\ Z_{ba} & Z_{bb} & Z_{bc} \\ Z_{ca} & Z_{cb} & Z_{cc} \end{bmatrix} \quad (53)$$

From (53), the symmetrical component matrix for an untransposed line can be computed (see [5]) using the symmetrical component transformation matrix and found to be the following:

$$Z_{\text{sym}} = \begin{bmatrix} Z_{00} & Z_{01} & Z_{02} \\ Z_{10} & Z_{11} & Z_{12} \\ Z_{20} & Z_{21} & Z_{22} \end{bmatrix} \quad (54)$$

Where:

$Z_{00}$  is the zero-sequence impedance.

$Z_{11}$  is the positive-sequence impedance.

$Z_{22}$  is the negative-sequence impedance.

$Z_{01}$  is the mutual impedance between the zero and positive sequences.

$Z_{02}$  is the mutual impedance between the zero and negative sequences.

$Z_{21}$  is the mutual impedance between the negative and positive sequences.

For a fully transposed line, the off-diagonal terms in (53) are the mutual impedances between conductors and are equal. For a transposed line with a flat line configuration, the self-impedances and self-admittances are equal and provide the equations derived in [5].

$$Y = \begin{bmatrix} Y_{\text{self}} & Y_{\text{mutual}} & Y_{\text{mutual}} \\ Y_{\text{mutual}} & Y_{\text{self}} & Y_{\text{mutual}} \\ Y_{\text{mutual}} & Y_{\text{mutual}} & Y_{\text{self}} \end{bmatrix} \quad (55)$$

$$Z = \begin{bmatrix} Z_{\text{self}} & Z_{\text{mutual}} & Z_{\text{mutual}} \\ Z_{\text{mutual}} & Z_{\text{self}} & Z_{\text{mutual}} \\ Z_{\text{mutual}} & Z_{\text{mutual}} & Z_{\text{self}} \end{bmatrix} \quad (56)$$

The symmetrical component matrix for the transposed line is shown in (57).

$$Z_{012} = \begin{bmatrix} Z_0 & 0 & 0 \\ 0 & Z_1 & 0 \\ 0 & 0 & Z_2 \end{bmatrix} \quad (57)$$

In the symmetrical component matrix, the diagonal terms  $Z_0$ ,  $Z_1$ , and  $Z_2$  are the zero-, positive-, and negative-sequence impedances of the transmission line, respectively. Note that the off-diagonal terms are zero and indicate that there is no coupling between the positive-, negative-, and zero-sequence networks for the transposed line. The method that relies on the calculation of the impedance based on sequence components is only valid for transposed lines; however, off-diagonal terms are often approximated as zero for untransposed lines.

### 3.3.1 Equivalent PI Circuit

Figure 18 shows the per-phase equivalent PI circuit of a three-phase transmission line [6].

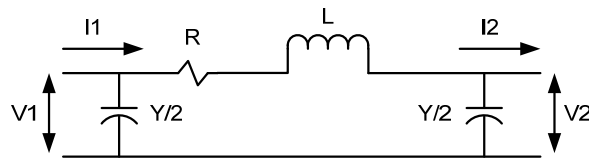


**Figure 18** Equivalent PI Circuit of a Three-Phase Transmission Line

The relationship between the currents and voltages is expressed using the following equations:

$$I_1 + I_2 = Y \cdot (V_1 + V_2) \quad (58)$$

$$V_1 - V_2 = Z \cdot I_d \quad (59)$$

Where:

$$I_d = I_1 - Y \cdot V_1 \quad (60)$$

### 3.3.2 Steady-State Distributed Line Parameters

Figure 19 shows the relationship between the current and voltage along the line in terms of the distributed parameters.

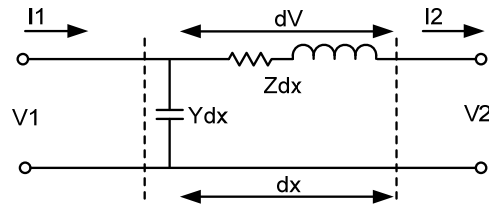


**Figure 19 Distributed Model of a Three-Phase Transmission Line**

Equation (61) defines the model of the distributed parameter line.

$$\frac{dV}{dx} = Z \cdot I \quad \frac{dI}{dx} = Y \cdot V \quad (61)$$

The solution of (61), in terms of the sending and receiving voltage and currents [6], is defined as follows:

$$\begin{bmatrix} V_1 \\ I_1 \end{bmatrix} = \begin{bmatrix} \cosh(\Gamma l) & \sinh(\Gamma l) Z_0 \\ Y_0 \sinh(\Gamma l) & Y_0 \cosh(\Gamma l) Z_0 \end{bmatrix} \begin{bmatrix} V_2 \\ I_2 \end{bmatrix} \quad (62)$$

Where:

$$\Gamma = (ZY)^{1/2}$$

$$Z_o = \Gamma Y^{-1} = \Gamma^{-1} Z$$

$$Y_o = Y \Gamma^{-1} = Z^{-1} \Gamma$$

### 3.3.3 Classification of Transmission Lines

Overhead lines can be classified according to length based on the approximations justified in their modeling [7]. They are classified as follows:

- Short lines are shorter than 50 miles. They have negligible shunt capacitance and may be approximated as series impedance.
- Medium lines have lengths in the range of 50 to 125 miles. They can be approximated by the equivalent PI circuit. The majority of lines fall under this category, and this model is suitable for our analysis.
- Long lines are longer than 125 miles. For these lines, the distributed effects of the parameters can be significant and need to be represented by the distributed line parameters.

## 3.4 Calculation of Parameters

### 3.4.1 General Overview

The proposed method uses synchronized PMUs to obtain the phase voltages and currents at both ends of a line. These devices must have accurate time information. GPS satellite-synchronized clocks with microsecond accuracy provide this information through demodulated IRIG B signals. Proper time synchronization allows for obtaining time-synchronized samples of voltages and currents for use in calculating the impedance and admittance matrices.



### 3.4.2 Transposed Lines

#### 3.4.2.1 Equivalent PI Circuit Analysis

A test setup using PSCAD/EMTDC software was used to simulate the conditions, and the setup validates the proposed solutions. Figure 20 shows the test setup for the line.

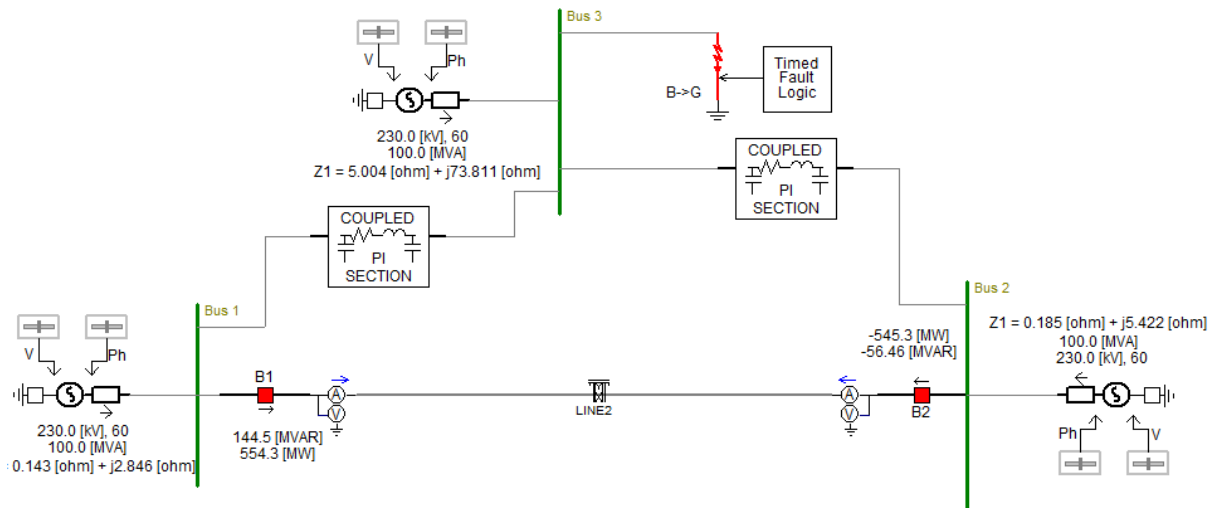


**Figure 20 PSCAD/EMTDC Test Setup and Model for Testing**

Because the line is transposed, there are three unknowns in the Y and Z matrices. Equations (64) and (65) can be used to solve for these parameters. One unbalanced condition seen by the line is required for the solution. This condition can be an external fault in the power system that generates enough zero-sequence voltage and current at the measurement locations. A measure for the unbalance is the ratio of positive-sequence current to zero-sequence current ( $I_0/I_1$ ). The simulation was done with a close-in fault, moving the fault location away from the line under study. Good results were achieved with an  $I_0/I_1$  ratio as low as 5 percent.

For the calculation of the Y matrix, when we define (63), (58) takes on the form of (64).

$$I = I_1 + I_2 \quad V = V_1 + V_2 \quad (63)$$

$$I = VY \quad (64)$$

The Y matrix can be determined using matrix inversion. Similarly, Id from (60) can be calculated. If we define  $V' = V1 - V2$ , (59) becomes the following:

$$V' = Id \cdot Z \quad (65)$$

The Z matrix can also be solved using matrix inversion.

### **3.4.2.2 Distributed Line Parameters**

For the distributed line parameters, (61) can be solved directly using numerical integration in the complex domain and a nonlinear iterative solution. Alternatively, (62) can be solved using a nonlinear iterative solution. The same line modeled in Figure 20 was used for the calculation.

### **3.4.2.3 Results**

Table 1 shows the line impedance comparison between the PSCAD/EMTDC simulation versus the equivalent PI circuit and distributed parameters.

**Table 1 Line Impedance Comparison for Transposed line**

<b>Calculation Method</b>	<b>Positive-Sequence Magnitude (Primary Ohms)</b>	<b>Positive-Sequence Angle (Degrees)</b>	<b>Zero-Sequence Magnitude (Primary Ohms)</b>	<b>Zero-Sequence Angle (Degrees)</b>
PSCAD/EMTDC Simulation Values	37.485	85.435	100.277	70.825
Equivalent PI Circuit	37.43	85.457	101.93	71.433
Distributed Parameters	37.536	85.444	101.868	71.324

A comparison between the equivalent PI circuit and distributed parameter calculations shows negligible difference, and both methods calculate the positive- and zero-sequence impedances accurately.

### 3.4.3 Untransposed Lines

Most transmission lines fall under this category, so developing a solution for untransposed lines is essential. The solution focuses on the equivalent PI circuit analysis. The distributed parameter line solution is complex and requires extensive calculation because there are 18

equations to solve iteratively. In the case of a fully transposed line, there is no significant difference between the two methods.

Because there are more unknowns in the  $Y$  and  $Z$  matrices for untransposed lines compared with transposed lines, three independent states from the power system are needed to solve (64) and (65).

The conditions to solve (64) and (65) require (65) to have full rank. This can be achieved by having one state based on load conditions and two other states with an unbalanced condition. Similar to the transposed lines, the unbalanced condition does not have to occur on the untransposed line; it can occur anywhere in the power system that can generate unbalance. A measure of  $I_0/I_1$  can indicate the amount of unbalance from the fault. Simulation results show even small unbalance (as low as 3 to 5 percent) can be used. The advantage of using three states (one from the load and two with unbalanced conditions) for the calculation is that remote faults in the system can be used for the calculation of the impedances and internal line faults are not required. The  $I$  and  $V$ , equations from (64) and (65) represent A-, B-, and C-phase currents and voltages from three different states. The solution for  $Y$  and  $Z$  uses the generalized (pseudo) inverse matrix operation, which gives the least squares solution [8].

Table 2 shows the line impedance comparison between the PSACAD/EMTDC simulation values versus the equivalent PI circuit.

**Table 2 Line Impedance Comparison for Untransposed Line**

<b>Calculation Method</b>	<b>Positive-Sequence Magnitude (Primary Ohms)</b>	<b>Positive-Sequence Angle (Degrees)</b>	<b>Zero-Sequence Magnitude (Primary Ohms)</b>	<b>Zero-Sequence Angle (Degrees)</b>
PSCAD/EMTD C Simulation Values	15.021	85.435	40.184	70.825
Equivalent PI Circuit	15.214	84.582	40.345	72.478

The results show that the calculation using the equivalent PI model for an untransposed line closely matches the actual line impedance used in the simulation.

### 3.5 Case Study

Entergy received a Smart Grid Investment Grant (SGIG) from the U.S. Department of Energy and installed PMUs on multiple lines of their system as part of the Entergy PMU Hardening Project. The goal was to leverage the achievements and experience of the existing prototype Entergy system of phasors and reshape it into a wide-area monitoring system ready for operation. A transmission line with the setup shown in Figure 21 was chosen to provide the data for this analysis. The untransposed line is 230 kV and 31 miles long. The PMUs installed are independent from the line protection. The data is retrieved and archived in a substation

computer. Figure 22 shows the setup and the requirements for the collection of data used in the calculation of relay parameters.

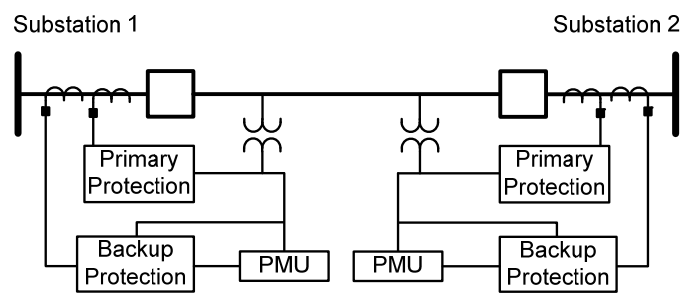


**Figure 21 PMU One-Line Diagram for the Case Study**

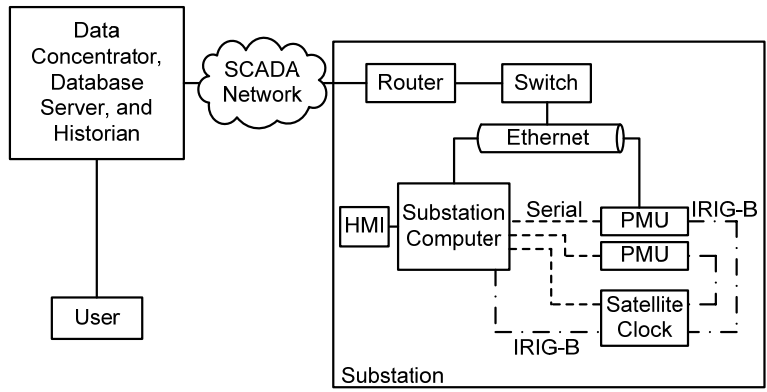


**Figure 22 PMUS Setup and Requirements**

Figure 23 through Figure 25 show example data collected from the PMUs from one of the states used for the calculation of the line impedance. The unbalance state was a B-phase-to-ground fault on the 230 kV system. Three-phase currents and voltages were captured from the synchrophasors showing the pre-fault, fault, and post-fault window.

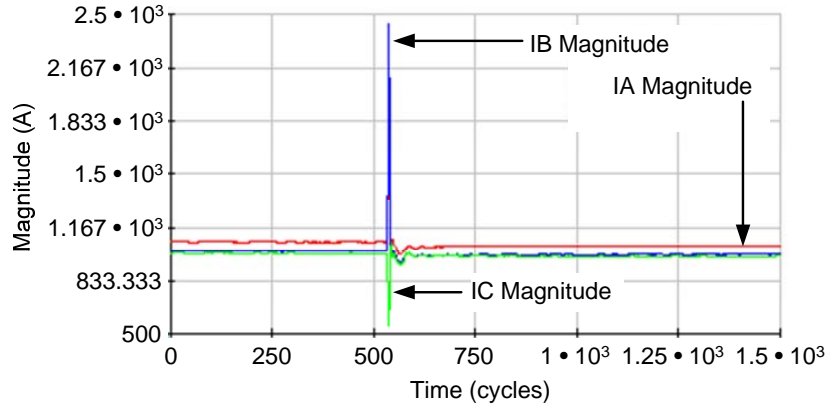


**Figure 23 Measured Currents From the PMUs During Prefault and Post-Fault Load Conditions and the Unbalance State**

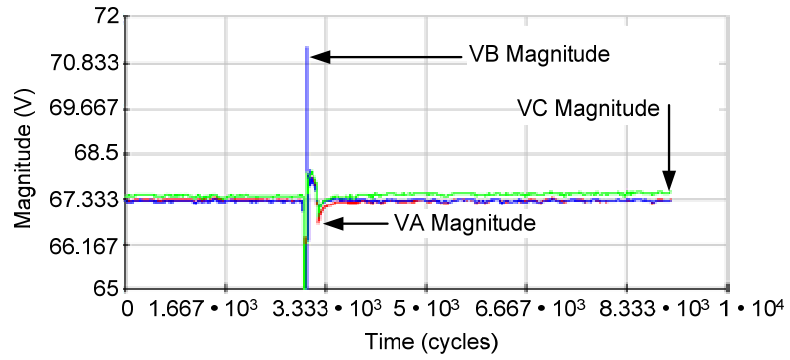


**Figure 24 Measured Voltages From the PMUs During Prefault and Post-Fault Load Conditions and the Unbalance State**

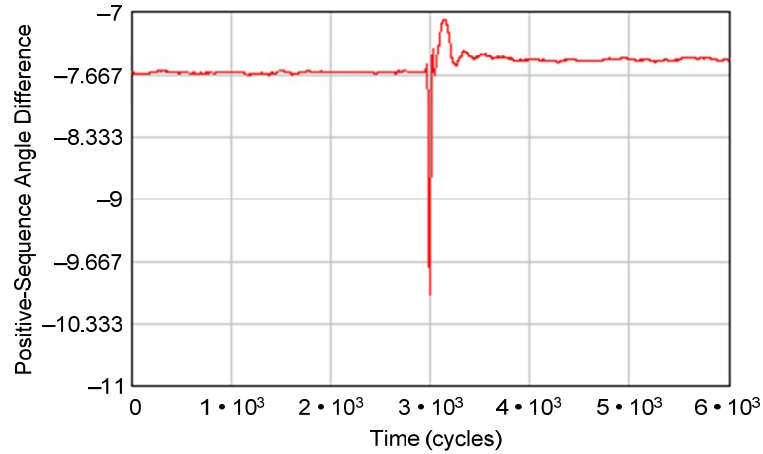
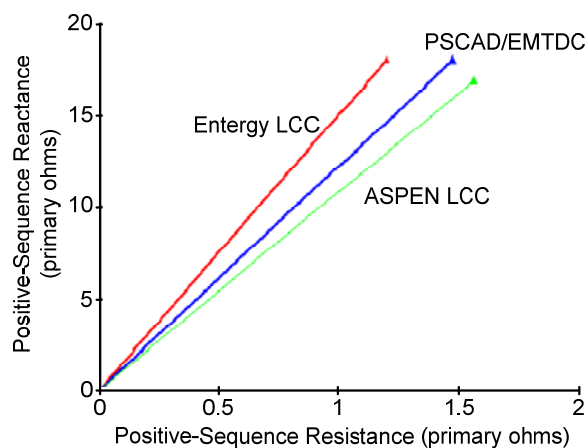


**Figure 25 Positive-Sequence Voltage Angle Difference Between the Two Stations From the PMUs During Prefault and Post-Fault Load Conditions and the Unbalance State**

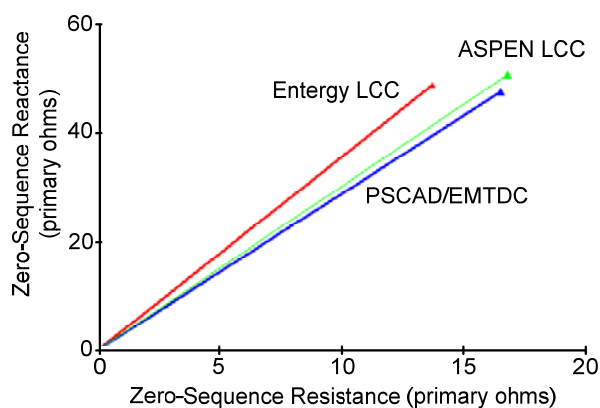
### 3.6 Case Study Results and Discussion

Figure 26 and Figure 27 compare the calculated line impedances from three different line constants calculation (LCC) programs: Entergy LCC, PSCAD/EMTDC, and ASPEN LCC. The Entergy LCC was used to develop the settings. There is a slight difference between the positive-sequence impedance and the zero-sequence impedance. This can be attributed to how the LCC programs internally calculate these values and the assumptions made.





**Figure 26 Comparison of the Positive-Sequence Impedance Vectors Calculated From the Three LCC Programs**



**Figure 27 Comparison of the Zero-Sequence Impedance Vectors Calculated From the Three LCC Programs**

Figure 28 and Figure 29 compare the calculated line impedance of the three LCC programs and the line impedance derived from the synchrophasor measurements. The positive-sequence impedance measured by the synchrophasors closely matches that from the Entergy LCC. The zero-sequence impedance differs from the LCC programs, specifically the magnitude. Its percentage of error is about 19 percent; however, the zero-sequence angle is within 6 percent.

This could be due to many factors, such as the earth resistivity assumption used in the LCC programs, CT errors, synchrophasor filtering and sampling, and fault duration that needs to be investigated further. However, the data is still useful for checking distance relay settings.

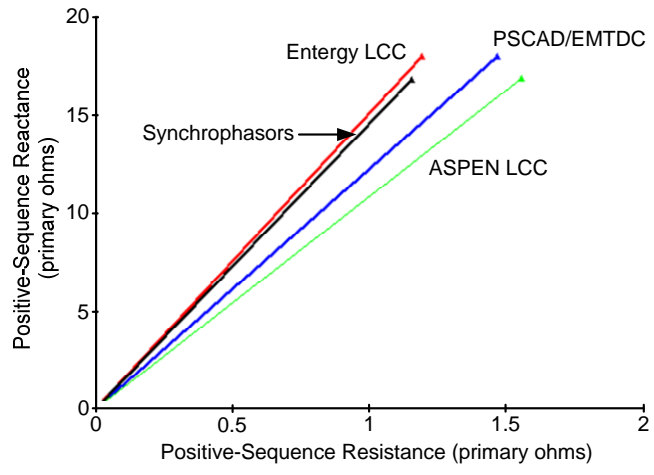


**Figure 28 Comparison of the Positive-Sequence Impedance Vectors Calculated From the**

**Three LCC Programs and Synchrophasors**

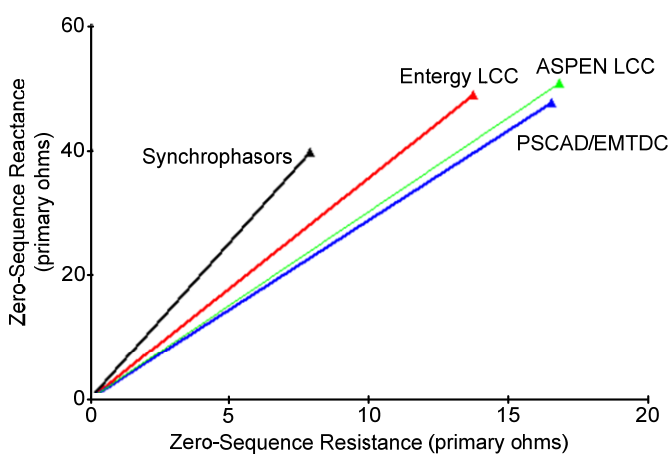


**Figure 29 Comparison of the Zero-Sequence Impedance Vectors Calculated From the Three LCC Programs and Synchrophasors**

Distance-based line protection uses positive-sequence impedance and a zero-sequence compensation factor  $k_0$ , along with voltage and current measurements, to determine if faults are inside the protection zone. One method to estimate the distance to the fault for A-phase-to-ground faults by mho elements is provided in (66) [9].

$$mAG = \frac{\text{Re}(V_a \cdot V_{pol}^*)}{\text{Re}(Z_{1L} \cdot (I_a + k_0 \cdot I_G) \cdot V_{pol}^*)} \quad (66)$$

Where:

$V_a$  is the faulted phase voltage.

$V_{pol}$  is the polarizing quantity.

$I_a$  is the faulted phase current.

$I_G$  is the residual current.

$Z_{1L}$  is the positive-sequence line impedance.

$k_0$  is the zero-sequence compensation factor.  $k_0 = \frac{Z_{0L} - Z_{1L}}{3Z_{1L}}$

The zero-sequence compensation factor is the parameter used for the ground distance relay calculation. Figure 30 compares the zero-sequence compensation factor vectors calculated from the three LCC programs and the synchrophasor-based method.

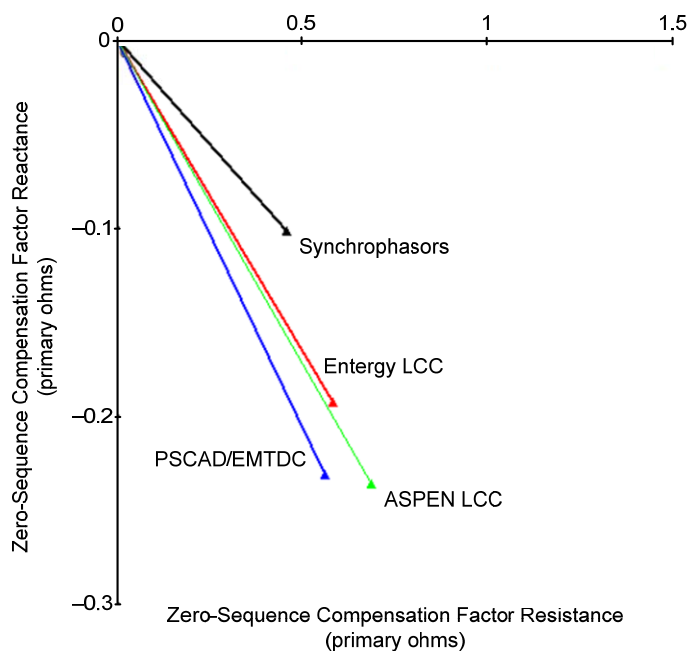


**Figure 30 Comparison of the Zero-Sequence Compensation Factor Vectors Calculated**

**From the**

**Three LCC Programs and Synchrophasors**

The effect of both the LCC zero-sequence compensation factor and synchrophasor zero-sequence compensation factor on the distance element reach for the ground fault can be analyzed using (66). The per-unit reach along the line for both zero-sequence compensation factors is calculated for comparison. Figure 31 shows the results for a fault current with 80 degrees lagging phase shift. The calculated Entergy LCC zero-sequence compensation factor reach at 80 percent of the line corresponds to a reach of 88 percent for the synchrophasor zero-sequence compensation factor. This result shows no overreach of the zone distance element.

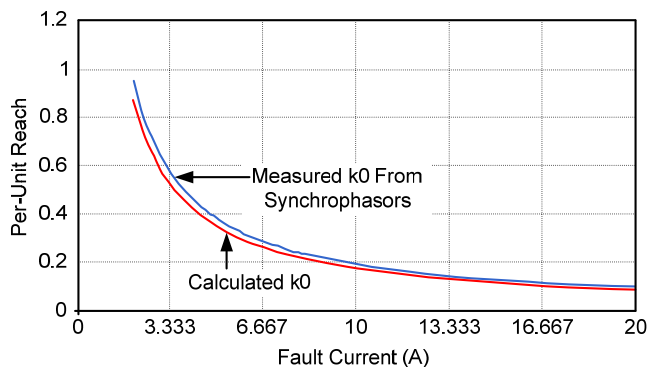


**Figure 31 Per-Unit Reach Versus Phase-to-Ground Fault Current Magnitude for Calculated Zero-Sequence Compensation Factors From Entergy LCC and Synchrophasors**

Table 3 through Table 7 provides the settings for a proposed method for checking the relay settings from the synchrophasor data. The tables summarize the actual in-service settings of interest in the relay and compare them with the values derived from the synchrophasors. A difference between the two values above a threshold can be used to indicate a discrepancy. The goal of this is to minimize errors in the settings that can cause undesired operations, such as distance element overreach or underreach. Zone 1 should never overreach the remote terminal, and Zone 2 should always overreach. For Zone 1, if the measured impedance is less than the set relay reach, the reach should not exceed 5 to 10 percent of the measured impedance. The tolerance can be smaller if Zone 1 is set to 90 percent of the line versus 80 percent. The checking limit can be different based on the settings and their impact on the operation of the relay.

The calculation for both positive- and zero-sequence impedances requires three conditions from the power system (one steady state and two unbalance states). The positive-sequence impedance can be determined first from a steady state when the line is first put in service. The

zero-sequence impedance can be estimated using historical data based on a ratio of positive-sequence impedance. Once the other two states of unbalance are made available by monitoring the  $I_0/I_1$  ratio, the calculations can be made for the validation and verification of relay settings based on the measurement.

**Table 3 Relay Transmission Line Parameters**

<b>Relay Setting (Secondary Ohms)</b>	<b>In-Service Relay Setting</b>	<b>Synchrophasor- Derived Values</b>	<b>Error (%)</b>	<b>Suggested Checking Method (%)</b>
Z1MAG	5.41	5.1	-5.73	Within $\pm 10$
Z1ANG	86.24	86.1	-0.16	Within $\pm 5$
Z0MAG	15.20	12.3	-19.08	Within $\pm 20$
Z0ANG	74.35	78.735	5.90	Within $\pm 10$

**Table 4 Phase Distance Zone Settings**

<b>Relay Setting (Secondary Ohms)</b>	<b>In-Service Relay Setting</b>	<b>Synchrophasor- Derived Values</b>	<b>Error (%)</b>	<b>Suggested Checking Method (%)</b>
Z1P	4.6	4.34	-5.73	Within $\pm 10$
Z2P	7.1	6.69	-5.73	Within $\pm 10$
Z3P	8.2	7.73	-5.73	Within $\pm 10$
Z4P	15	14.14	-5.73	Within $\pm 10$

**Table 5 Ground Distance Zone Settings**

<b>Relay Setting (Secondary Ohms)</b>	<b>In-Service Relay Setting</b>	<b>Synchrophasor- Derived Values</b>	<b>Error (%)</b>	<b>Suggested Checking Method (%)</b>
Z1MG	4.6	4.34	-5.73	Within $\pm 10$
Z2MG	7.1	6.69	-5.73	Within $\pm 10$
Z3MG	8.2	7.73	-5.73	Within $\pm 10$
Z4MG	15	14.14	-5.73	Within $\pm 10$



**Table 6 Zero-Sequence Compensation Factor**

<b>Relay Setting (Secondary Ohms)</b>	<b>In-Service Relay Setting</b>	<b>Synchrophasor- Derived Values</b>	<b>Error (%)</b>	<b>Suggested Checking Method</b>
k01M	0.613	0.5	-18.43	Within $\pm 0.1$ ohms
k01A	-18.30	-12.527	-31.55	Within $\pm 5$ degrees

**Table 7 Directional Element Settings**

<b>Relay Setting (Secondary Ohms)</b>	<b>In-Service Relay Setting</b>	<b>Synchrophasor- Derived Values</b>	<b>Error (%)</b>	<b>Suggested Checking Method (%)</b>
Z2F	2.71	2.55	-5.90	Within $\pm 10$
Z2R	2.81	2.65	-5.69	Within $\pm 10$

### 3.7 Conclusion

This paper presents a method to calculate the positive- and zero-sequence impedances for transposed and untransposed transmission lines using PMUs. These calculations are used to verify distance relay settings. The method for checking these calculations is presented along with the PMU data required for the calculation and system conditions. The advantage of using this method to validate the settings is that it does not require additional changes to the line or

conducting any tests or outages, as long as the line has a PMU that collects three-phase voltages and currents.

Further investigation is required to verify the accuracy of this method compared with the LCC-derived settings. If there is a fault on the line with a known fault location, the performance of a relay based on the LCC-derived settings and synchrophasors can be used to determine which method is more accurate. Another area of investigation is analyzing the effects that CTs, filtering, sampling, and fault duration can have on the suggested validation method.

### **3.8 Comments**

- Percent error was used to calculate the relative error for both magnitude and phase angle. Distance relays are set as a percentage of the transmission line impedance. The effective impedance values calculated from the measured data fall in a narrow range (70-85 degree), and using relative error provides a useful indication of errors for comparison to determine if distance relays will overreach or underreach, whereas absolute error lacks this information.
- The effect of temperature and frequency on errors was not considered. Measurement data is captured during steady state, and filtering extracts the fundamental frequency so no higher frequencies are present in the data. Temperature change on the measurement data is small, and distance relays are set with a margin to account for such errors.
- A method was provided in this paper to validate distance relay settings by providing a suggested checking method. This method checks if the percent error between existing

settings and measured settings falls within a range. This range is wide to allow a higher margin without nuisance reports. In the case of errors outside this range these settings can be flagged for further review by the settings engineer. Review of transmission line configuration, conductor properties and mutual coupling can be used to further check the line parameters and determine if the synchrophasor derived values can overwrite existing settings.

## Chapter 4 RTDS Validation Testing

### 4.1 Test Setup

The structure of the network developed for validation testing is shown in Figure 32

The main components of the test setup are:

- Power system: A power system simulated in a RTDS real-time simulator is used to generate the voltage and current signals. The RTDS can produce low-level analog signals that can be injected into the PMUs.
- Satellite clock: An SEL-2407<sup>®</sup> Satellite-Synchronized Clock with an antenna is used to generate time reference signals. The time reference is provided to the PMUs via its IRIG-B output channel.
- PMUs: Two SEL-421 Protection, Automation, and Control System relays with PMU functionality are used as PMUs. They collect analog information from the power system network simulated in the RTDS through analog outputs, measure synchrophasors, add time stamps, and stream real-time data using the IEEE C37.118-2005 Standard for Synchrophasors protocol [26].
- Data network: The synchrophasor network uses a TCP/IP network for data transmission. The 100 Mbps communications links are connected through a network switch shared with the RTDS simulator and other computers in the lab.
- PDC: A PC running SEL-5073 SYNCHROWAVE<sup>®</sup> Phasor Data Concentrator (PDC) Software collects synchrophasor information coming from different PMUs, aligns the data according to time stamps, and sends the collated measurements to application programs using the synchrophasor protocol through the 100 Mbps data network.

- Client Program: SEL-5078-2 SYNCHROWAVE® Central Visualization and Analysis Software is a data visualization program that interfaces with the PDC.

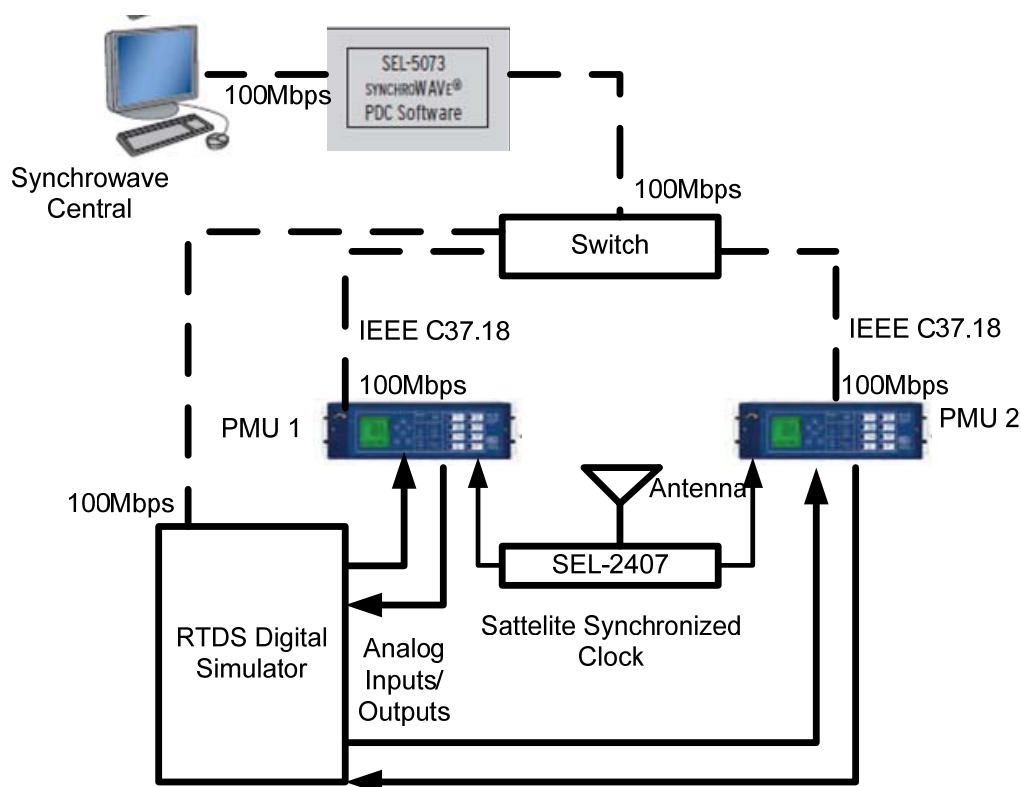


**Figure 32 Experimental Network Set Up**

## 4.2 RTDS and Power System Overview

### 4.2.1 RTDS Overview

The real-time digital simulator used in this research is manufactured by RTDS Technologies, Inc. [21] and is comprised of optimized hardware and software to run an electromagnetic transient simulation in real time. RTDS is a powerful tool used to test equipment in real time. The software that allows creation of simulations and acts as the interface between the RTDS simulator and the user is called RSCAD. The DRAFT module of RSCAD software facilitates the setting up of simulations using the component models included in its component library.

The component library includes most of the models required to simulate power systems, control systems, and protection and automation systems. RSCAD software allows the user to build the simulation case and input the parameters of each component. RSCAD runs on a normal PC, and once the simulation case is built and compiled, it is downloaded to the RTDS simulator. The RTDS simulator is a parallel computer optimized for power system simulation and can solve the differential equations that describe the simulated power system at a speed faster than the physical phenomena being modeled. Since the solution is real time, it can be directly interfaced with physical devices such as digital relays [25]. This is facilitated via its analog and digital outputs. RTDS can also take digital and analog signals as inputs. There are separate hardware input/output boards that facilitate interfacing with physical devices. It is also possible to interact with the simulation in real time using the RUN TIME module in the RSCAD software.

#### **4.2.2 Power System Overview**

The EMTDC/PSCAD model shown in Figure 33 was used and modeled in the RTDS draft component to simulate the currents and voltages to be injected into the PMUs.

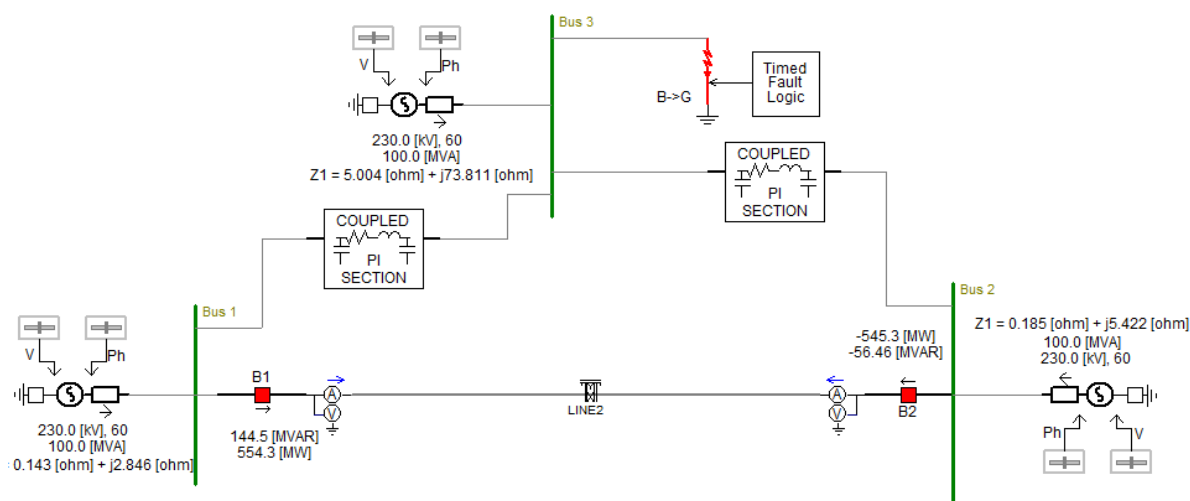


**Figure 33 Power System Modeled in RTDS**

### 4.3 Configuration and Description of the Network Equipment

In this section, a description of the SEL-421 is presented along with the main settings and parameters used to configure this device.

#### 4.3.1 Description of the Synhrophasor

The SEL-421 is a multifunctional relay used for power system protection, automation, and control applications. Among all functionalities, this relay can protect dual breaker transmission lines using distance, directional overcurrent, instantaneous overcurrent, and time-overcurrent elements. It also has synchrophasor capability that will be utilized for the real-time digital simulation. It is possible to acquire synchrophasor measurements from SEL-421 when a high-accuracy time source, such as a GPS clock, is connected to the device. It also supports C37.118-2005 [26] [27]. As mentioned, this relay has the capability to receive signals using the low-level interface connection.

### 4.3.2 SEL-421 Global Settings

The global settings in the SEL-421 set parameters such as location, identification, nominal frequency, number of setting groups, and enabling and configuring synchrophasor measurements. The global settings used in the two relays set up to collect synchrophasor data are provided in the figures below.

The image shows a configuration interface for PMU Global Settings. It consists of several sections with dropdown menus and labels:

- EPMU Enable Synchronized Phasor Measurement:** A dropdown menu with the value 'Y' selected. The label indicates 'Select: Y, N'.
- Synchronized Phasor Measurement:** A section header.
- MFRMT Message Format:** A dropdown menu with the value 'C37.118' selected. The label indicates 'Select: C37.118, FM'.
- MRATE Messages per Second:** A dropdown menu with the value '30' selected. The label indicates 'Select: 1, 2, 4, 5, 10, 12, 15, 20, 30, 60'.
- PMAPP Type of PMU Application:** A dropdown menu with the value 'N' selected. The label indicates 'Select: F, N'.
- NUMPHDC Number of Data Configurations:** A dropdown menu with the value '1' selected. The label indicates 'Select: 1-5'.
- PMTRIG Trigger (SELogic):** A text field containing the value 'RB01 OR 50G1 OR 50Q1'.

**Figure 34 PMU Global Settings**



PMSTN1 Station Name (16 characters)	STATIONA
PMID1 PMU Hardware ID	1 Range = 1 to 65534
PHNR1 Phasor Numerical Representation	I Select: I, F
PHFMT1 Phasor Format	P Select: R, P
FNR1 Frequency Numerical Representation	I Select: I, F
PHDV1 Phasor Data Set, Voltages	ALL Select: V1, PH, ALL
PHDI1 Phasor Data Set, Currents	ALL Select: I1, PH, ALL

**Figure 35 Additional PMU Global Settings**

### 4.3.3 Port 5 settings

The settings for Port 5 are as follows:

EPMIP Enable C37.118 Communications	Y Select: Y, N
<b>PMU Output Configuration 1</b>	
PMOTS1 PMU Output 1 Transport Scheme	TCP Select: OFF, TCP, UDP_S, UDP_T, UDP_U
PMODC1 PMU Output 1 Data Configuration	1 Select: 1-5
PMOIPA1 PMU Output 1 Client IP (Remote) Address	192.168.0.104
PMOTCP1 PMU Output 1 TCP/IP (Local) Port Number	4712 Range = 1025 to 65534
PMOUDP1 PMU Output 1 UDP/IP Data (Remote) Port Number	4713 Range = 1025 to 65534

**Figure 36 Port Settings**

#### 4.3.4 Phasor Data Concentrator

In this section, a description of the SEL-5073 is presented along with the main settings and parameters used to configure the device in the synchrophasor network.

#### 4.3.5 Description of the SEL-5073 PDC

The PDC used in this research is the SEL-5073 from Schweitzer Engineering Laboratories, Inc. (SEL). SEL also offers a hardware PDC, but the software PDC was used for the laboratory synchrophasor network for ease of set up and the convenience of using my own PC, where reliability is not as critical. SEL-5073 functions as a data collector because it gathers data coming from different devices, such as PMUs or other PDCs. Then, the SEL-5073 correlates the data based on time tags and retransmits the time-correlated data at a maximum rate of 240 messages per second [20]. The SEL-5073 can receive synchrophasor messages through Ethernet or serial communication, process incoming data from more than 500 PMUs, and transmit the correlated data over Ethernet to six outputs. The output data streams can be used for monitoring, control, and protection applications, as well as for data archiving. The internal architecture of the SEL-5073 and the interaction between the PDC and the PDC Assistant (user interface for PDC) is illustrated in Figure 37 [20].

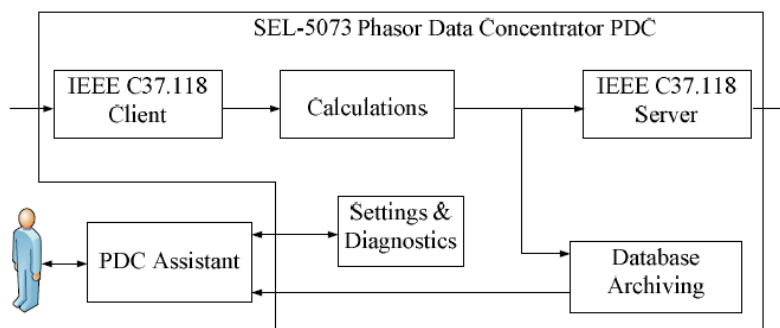


**Figure 37 SEL-5073 PDC Internal Architecture**

The main features of the SEL-5073 are [20]:

- High performance: Connects up to 500 PMUs or other PDCs at rates from 1 to 240 messages per second. The maximum 240 message per second can be supported with reduced number of inputs and outputs. It can support six separate outputs.
- Easy configuration and commission: Outputs, inputs, and archiving can be accomplished without interruption of the existing configuration.
- Synchrophasor message inputs and outputs: Serial or Ethernet communication can be used to read inputs according C37.118, and Ethernet is used to send out synchrophasor data in accordance to the above mentioned standard. Message rate and phasors can be selected individually for each output through the PDC Assistant software.
- Archiving: Data can be archived continuously or for a specific event. Pre- and post-disturbance data can be archived in different formats, such as binary, Comtrade, and comma separated values (CSV).
- Calculations: Real and reactive power, sequence components, algebraic calculations, and other calculations can be performed, and the results can be sent through the available outputs to other PDCs or applications programs.

#### **4.3.6 Settings for the SEL-5073**

The software used to configure the SEL-5073 is called PDC Assistant. It is possible to set inputs, outputs, and calculations and configure the archives using the PDC Assistant software. Another important feature of PDC Assistant is the real-time display, which shows the status of the PMUs. As PDC Assistant has the ability to archive data, it can also retrieve information based on the archived files, which is important for post-mortem analysis. PDC Assistant allows retrieving specific time data or for a specific event. PDC Assistant can run on the same

computer as the PDC software or can run from a different computer. There are four main categories of setting namely input settings, output settings, calculation settings, and archiving settings. Figure 38 presents the input settings used for STATIONA.

The screenshot displays the configuration window for a PMU named 'STATIONA'. The configuration includes the following fields:






- Enabled:**
- Station Name:** STATIONA
- Station Name Alias:** (empty)
- PMU ID:** 1
- PMU ID Alias:** (empty)
- Data Rate:** 30 Msg per sec
- Primary Connection:**
  - Physical Layer:** Ethernet
  - Transport Protocol:** TCP
  - IP Address:** 192.168.0.203
  - Port:** 4712
  - Local IP Address:** 192.168.0.104


Below the configuration fields is a table titled 'Expected Input Tags' with the following data:

Tag	Alias	Description	Units	Type	Quantity Type	Phase
V1YPM			V	Phasor	Voltage	
VAYPM			V	Phasor	Voltage	
VBYPM			V	Phasor	Voltage	
VCYPM			V	Phasor	Voltage	
I1WPM			A	Phasor	Current	
IAWPM			A	Phasor	Current	
IBWPM			A	Phasor	Current	
ICWPM			A	Phasor	Current	

**Figure 38 PDC Input Configuration**

Figure 39 shows the output data settings from the PDC.

 Add Output
  Copy
  Paste
  Export
  Delete

 Output

**Output: Output**

Enabled

Output Name

PDC ID

Data Rate  Msg per sec

Waiting Period  ms

Phasor Domain

**Connection Settings**

Transport Protocol

Port

Local IP Address

STATIONA	STATIONA	V1YPM	30	V	Phasor	Voltage
STATIONA	STATIONA	VAYPM	30	V	Phasor	Voltage
STATIONA	STATIONA	VBYPM	30	V	Phasor	Voltage
STATIONA	STATIONA	VCYPM	30	V	Phasor	Voltage
STATIONA	STATIONA	I1WPM	30	A	Phasor	Current
STATIONA	STATIONA	IAWPM	30	A	Phasor	Current
STATIONA	STATIONA	IBWPM	30	A	Phasor	Current
STATIONA	STATIONA	ICWPM	30	A	Phasor	Current
STATIONB	STATIONB	V1YPM	30	V	Phasor	Voltage
STATIONB	STATIONB	VAYPM	30	V	Phasor	Voltage
STATIONB	STATIONB	VBYPM	30	V	Phasor	Voltage
STATIONB	STATIONB	VCYPM	30	V	Phasor	Voltage
STATIONB	STATIONB	I1WPM	30	A	Phasor	Current

STATIONB	STATIONB	I	AWPM	30	A	Phasor	Current
STATIONB	STATIONB	I	BWPM	30	A	Phasor	Current
STATIONB	STATIONB	I	CWPM	30	A	Phasor	Current

**Figure 39 PDC Output Configuration**

To increase accuracy in concentrating data, the SEL-5073 uses a scheme that discards data with unusual timestamps. The algorithm looks at the timestamps of all the inputs and performs a simple scheme to determine timestamps that are earlier or later than the other timestamps received. This ensures that data coming in with an erroneous timestamp does not corrupt data with valid timestamps.

Archiving settings allow selection between continuous archiving and trigger-based archiving. If trigger-based archiving is selected, settings allow to specify triggered event(s), the pre-trigger and post-trigger record durations, the maximum number of events, and retention of the archives. Additional archiving settings include specifying the data rate format, archive retention, name of the archive, and data rate. This information can be retrieved in polar or rectangular phasor format, in degrees or radians, and the file can be CSV, Binary Comtrade, or ASCII Comtrade. The archiving scheme selected to get the data uses triggered archives that are triggered in the PMU either manually or via the 50G1 or 50Q1. 50G1 is residual ground picked up, and 50Q1 is negative-sequence picked up. These elements will pick up when there is unbalance in the power system, thus triggering the collection of synchrophasors. This method was chosen so the computer hard drive was not filled with data if continuous archiving was selected. Figure 40 shows the archiver settings.

Triggered Archive: Archive	
Archive Enabled	<input checked="" type="checkbox"/>
Archive Name	Archive
Waiting Period	1000 ms
Storage Estimate	0.03 GB
Pre-trigger Duration	1 Minutes
Post-trigger Duration	2 Minutes
Max Events	1
Archive Retention	1 Days
Ridethrough	1 Minutes

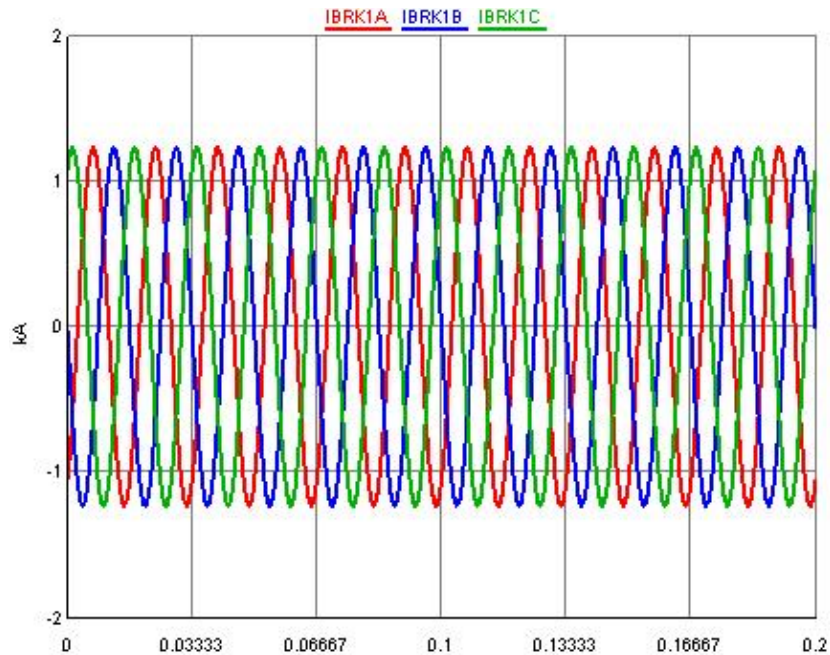
**Figure 40 PDC Archiver Configuration**

Once the data is archived, it is saved as a CSV file. This file is read directly in Mathcad and calculations are run to calculate the Y admittance and Z series impedance.

#### **4.4 Verification of the Test System During Steady State**

This section presents a test performed during steady state to verify the correctness of the measurements obtained through the synchrophasor network. The objective is to verify that all components in the synchrophasor network are properly configured and parameter settings are correct. Also, it tests that the measured quantities simulated in the RTDS are properly injected into the PMUs and retrieved via the PDC. The SEL-5078 software is used to compare these values.

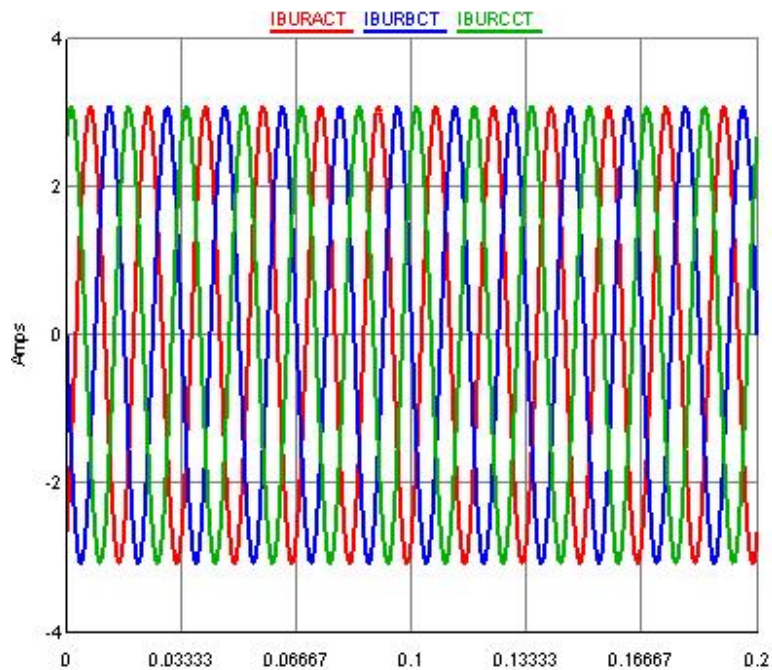
Figure 41 shows the primary current from Breaker 1 in the RTDS-simulated power system during a steady state load condition. The current is around 1,200 A.



**Figure 41 Primary Currents Simulated in the RTDS**

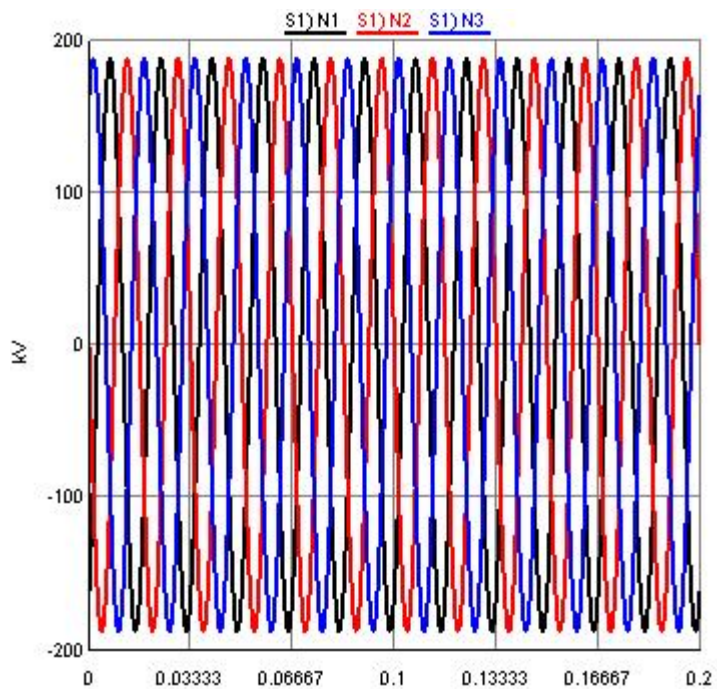
Figure 42 shows the CT secondary current. The CT ratio is set to 2000/5 so that the secondary current is 3 A secondary.





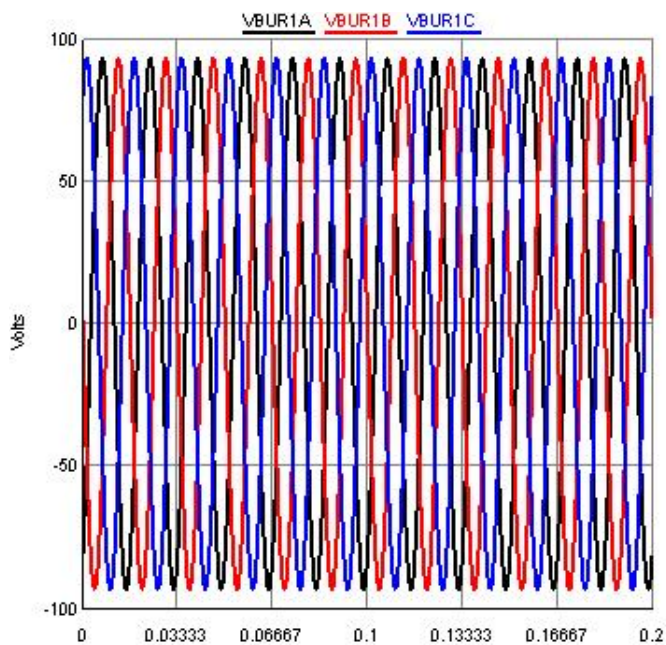
**Figure 42 Secondary Currents Simulated in the RTDS**

Figure 43 shows the primary voltage from Bus 1 in the RTDS-simulated power system during a steady state load condition. The voltage is 186 kV primary.



**Figure 43 Primary Voltage Simulated in the RTDS**

Figure 44 shows the PT secondary voltage. The PT ratio is set to 2000:1 so the secondary voltage is 90 V secondary.



**Figure 44 Secondary Voltages Simulated in the RTDS**

Figure 45 and Figure 46 show the relay measurements from injected RTDS signals described above. The values from the RTDS are in peak measurements. The relay filters the data and extracts fundamental RMS values. Therefore, the current seen by the relay should be:

$$1200/\sqrt{2} = 850 \quad (67)$$

And the voltage should be:

$$186000/\sqrt{2} = 132000 \quad (68)$$

The relay measurements confirmed the injected signal values and the settings entered for the CT ratio and PT ratio.

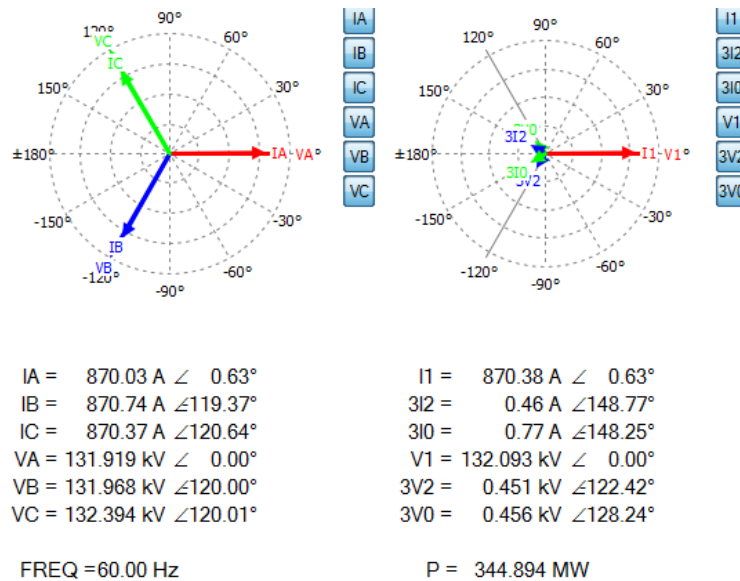


**Figure 45 PMU Metering Screen Capture**

Synchrophasor Metering Values				
Sigurd Line			Date: 10/22/2014 Time: 19:50:39.000	
RED BUTTE SUB			Serial Number: 1132040383	
Time Quality	Maximum time synchronization error:			0.000 (ms) TSOK = 1
Serial Port Configuration Error: N			PMU in TEST MODE = N	
Synchrophasors				
	VY Phase Voltages			VY Pos. Sequence Voltage
	VA	VB	VC	V1
MAG (kV)	131.966	132.014	132.442	132.141
ANG (DEG)	5.550	-114.464	125.552	5.546
	VZ Phase Voltages			VZ Pos. Sequence Voltage
	VA	VB	VC	V1
MAG (kV)	0.001	0.002	0.003	0.002
ANG (DEG)	-117.406	-169.683	70.761	-59.836
	IW Phase Currents			IW Pos. Sequence Current
	IA	IB	IC	I1W
MAG (A)	870.235	870.848	870.930	870.671
ANG (DEG)	6.175	-113.845	126.165	6.165

**Figure 46 PMU Synchrophasors Values Screen Capture**

The synchrophasor data from the PMUs is collected via the PDC. Figure 47 shows the status of the PMU and confirmation of the signals injected is received by the PDC for archiving and visualization tools.

Input Connections					
Name	PDC ID	Connection State	Time Quality	Received Data Frames	
STATIONA	1	Receiving Data	Normal	111473	
STATIONB	2	Receiving Data	Normal	111034	

Input PMUs					
PMU Name	PMU ID	Input Connection	PMU State	PMU Status	Unlock Time
STATIONA	1	STATIONA	Found	OK	Locked

Timestamp 10/23/2014 02:52:08.566    Frequency 60.001 Hz    df/dt 0.000 Hz./s

Phasors			Analogs	Digitals <input checked="" type="checkbox"/> = Nominal
Name	Magnitude	Angle		
V1YPM	132138.002	48.839		
VAYPM	131982.359	48.845		
VBYPM	132000.669	-71.161		
VCYPM	132440.120	168.828	(None)	(None)
I1WPM	870.715	49.475		
IAWPM	871.997	49.492		
IBWPM	869.861	-70.445		
ICWPM	870.288	169.384		

STATIONB	2	STATIONB	Found	OK	Locked
----------	---	----------	-------	----	--------

**Figure 47 PDC Screen Capture Receiving PMU Data**

Figure 48 shows the visualization of the current magnitude, voltage magnitude, and voltage angle between the two terminals using the SEL-5078 during a steady state load condition. These measurements are updated continuously at a message rate of 30 messages per second. The data captured is consistent with the values injected from the RTDS and is noise free, showing good data.



Figure 48 Visualization Software for PMU Data

### 4.5 RTDS Test Results

Several tests were conducted using the RTDS for both transposed and untransposed transmission lines of different line lengths and tower configurations. The following are the results from these tests.

## 4.5.1 Transposed Lines

### 4.5.1.1 Horizontal Tower Configuration

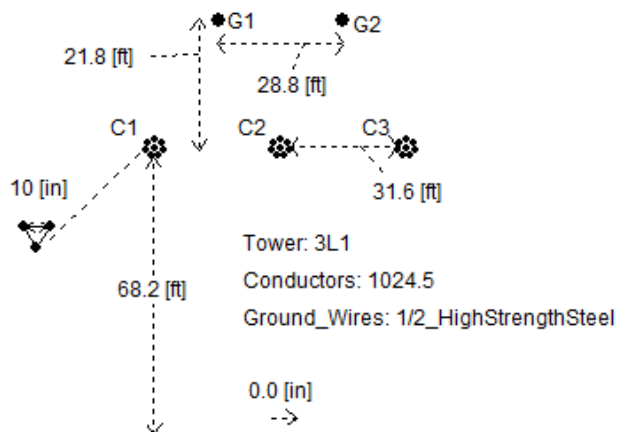


**Figure 49 Horizontal Tower Properties**

The tables below provide the results for the horizontal tower configuration in Figure 49 with a resistivity of 10 ohm meter for short, medium, and long lines.

**Table 8 Results for Short Transmission Line**

<b>Calculation Method</b>	<b>Positive-Sequence Magnitude (Primary Ohms)</b>	<b>Positive-Sequence Angle (Degrees)</b>	<b>Zero-Sequence Magnitude (Primary Ohms)</b>	<b>Zero-Sequence Angle (Degrees)</b>
RTDS Simulation Values	6.033	85.435	16.138	70.825
Synchrophasor-Derived Values	6.02	86.349	16.439	72.037
Percent Error	0.215%	1.070%	1.865%	1.711%



**Table 9 Results for Medium Transmission Line**

<b>Calculation Method</b>	<b>Positive-Sequence Magnitude (Primary Ohms)</b>	<b>Positive-Sequence Angle (Degrees)</b>	<b>Zero-Sequence Magnitude (Primary Ohms)</b>	<b>Zero-Sequence Angle (Degrees)</b>
RTDS Simulation Values	30.163	85.435	80.69	70.825
Synchrophasor-Derived Values	30.198	86.36	82.917	72.253
Percent Error	0.116%	1.083%	2.760%	2.016%

**Table 10 Results for Long Transmission Line**

Calculation Method	Positive-Sequence Magnitude (Primary Ohms)	Positive-Sequence Angle (Degrees)	Zero-Sequence Magnitude (Primary Ohms)	Zero-Sequence Angle (Degrees)
RTDS Simulation Values	90.49	85.435	242.071	70.825
Synchrophasor-Derived Values	90.279	86.336	243.426	72.443
Percent Error	0.233%	1.055%	0.560%	2.285%

**4.5.1.2 Vertical Tower Configuration**

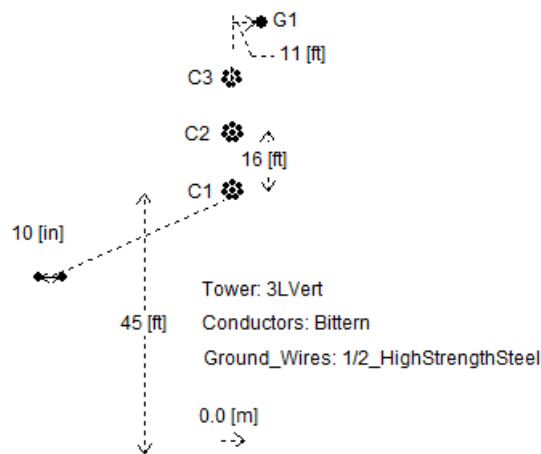


**Figure 50 Vertical Tower Properties**

The tables below provide the results for the vertical tower configuration in Figure 50 with a resistivity of 150 ohm meter for short, medium, and long lines.

**Table 11 Results for Short Transmission Line**

<b>Calculation Method</b>	<b>Positive-Sequence Magnitude (Primary Ohms)</b>	<b>Positive-Sequence Angle (Degrees)</b>	<b>Zero-Sequence Magnitude (Primary Ohms)</b>	<b>Zero-Sequence Angle (Degrees)</b>
RTDS Simulation Values	5.684	84.885	21.195	72.173
Synchrophasor-Derived Values	5.677	85.772	21.542	73.327
Percent Error	0.123%	1.045%	1.637%	1.599%

**Table 12 Results for Medium Transmission Line**

<b>Calculation Method</b>	<b>Positive-Sequence Magnitude (Primary Ohms)</b>	<b>Positive-Sequence Angle (Degrees)</b>	<b>Zero-Sequence Magnitude (Primary Ohms)</b>	<b>Zero-Sequence Angle (Degrees)</b>
RTDS Simulation Values	28.418	84.885	105.974	72.173
Synchrophasor-Derived Values	28.416	85.752	108.9944	73.427
Percent Error	0.007%	1.021%	2.850%	1.737%

**Table 13 Results for Long Transmission Line**

<b>Calculation Method</b>	<b>Positive-Sequence Magnitude (Primary Ohms)</b>	<b>Positive-Sequence Angle (Degrees)</b>	<b>Zero-Sequence Magnitude (Primary Ohms)</b>	<b>Zero-Sequence Angle (Degrees)</b>
RTDS Simulation Values	85.253	84.885	317.923	72.173
Synchrophasor-Derived Values	85.07	85.719	321.633	72.296
Percent Error	0.215%	0.983%	1.167%	0.170%

#### 4.5.1.3 Discussion and Summary of Results

Figures 50 and 51 show a summary graph of the results for the transposed transmission lines.

The results for the transposed line cases of different tower configuration and ground resistivity are consistent. The percent error does not exceed 5 percent. These results validate the proposed method to be used for checking relay settings.

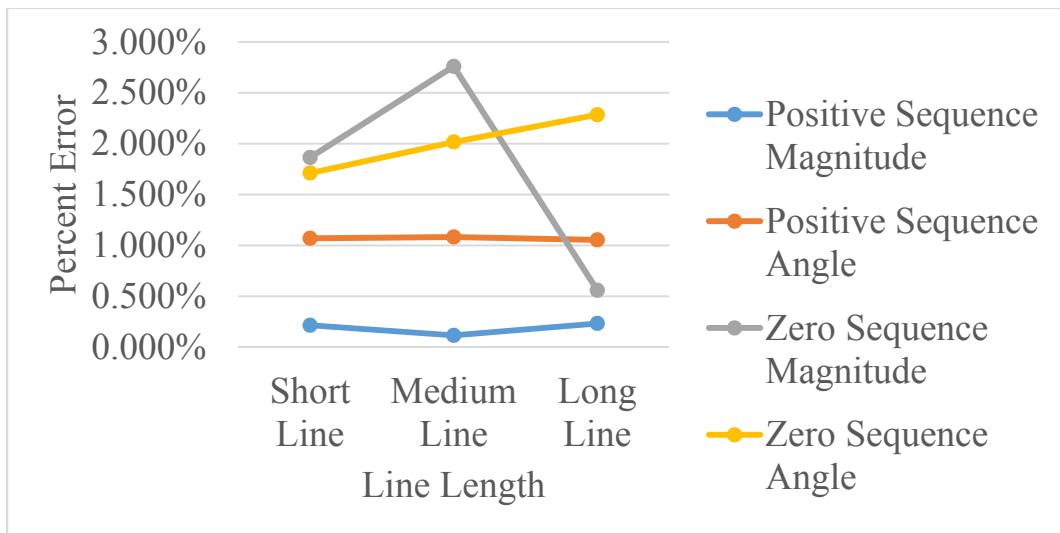


**Figure 51 Horizontal Tower Configuration Results**

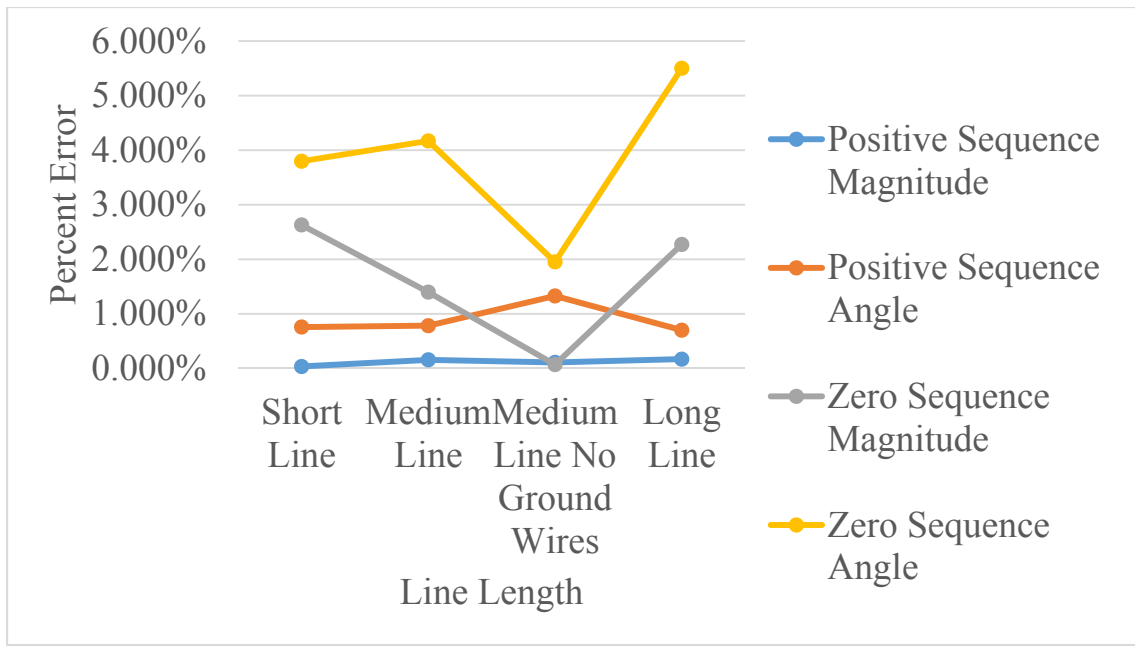


**Figure 52 Vertical Tower Configuration Results**

**4.5.2 Untransposed Lines**

**4.5.2.1 Horizontal Tower Configuration**

The tables below provide the results for the horizontal tower configuration in Figure 49 with a resistivity of 10 ohm meter for short, medium, and long lines.

**Table 14 Results for Short Transmission Line**

<b>Calculation Method</b>	<b>Positive-Sequence Magnitude (Primary Ohms)</b>	<b>Positive-Sequence Angle (Degrees)</b>	<b>Zero-Sequence Magnitude (Primary Ohms)</b>	<b>Zero-Sequence Angle (Degrees)</b>
RTDS Simulation Values	6.033	85.435	16.138	70.825
Synchrophasor-Derived Values	6.035	86.081	16.562	73.513
Percent Error	0.033%	0.756%	2.627%	3.795%



**Table 15 Results for Medium Transmission Line**

<b>Calculation Method</b>	<b>Positive-Sequence Magnitude (Primary Ohms)</b>	<b>Positive-Sequence Angle (Degrees)</b>	<b>Zero-Sequence Magnitude (Primary Ohms)</b>	<b>Zero-Sequence Angle (Degrees)</b>
RTDS Simulation Values	30.163	85.435	80.69	70.825
Synchrophasor-Derived Values	30.116	86.103	81.817	73.777
Percent Error	0.156%	0.782%	1.397%	4.168%

**Table 16 Results for Long Transmission Line**

<b>Calculation Method</b>	<b>Positive-Sequence Magnitude (primary ohms)</b>	<b>Positive-Sequence Angle (degrees)</b>	<b>Zero-Sequence Magnitude (primary ohms)</b>	<b>Zero-Sequence Angle (degrees)</b>
RTDS Simulation Values	90.49	85.435	242.071	70.825
Synchrophasor Derived Values	90.337	86.032	247.569	74.719
Percent Error	0.169%	0.699%	2.271%	5.498%

Table 17 shows the results of the same horizontal tower with no ground wires present. The line is untransposed.

**Table 17 Results for Medium Untransposed Transmission Line No Ground Wires**

<b>Calculation Method</b>	<b>Positive-Sequence Magnitude (Primary Ohms)</b>	<b>Positive-Sequence Angle (Degrees)</b>	<b>Zero-Sequence Magnitude (Primary Ohms)</b>	<b>Zero-Sequence Angle (Degrees)</b>
RTDS Simulation Values	30.206	85.722	90.333	80.103
Synchrophasor-Derived Values	30.173	86.86	90.27	81.665
Percent Error	0.109%	1.328%	0.070%	1.950%

#### **4.5.2.2 Vertical Tower Configuration**

The tables below provide the results for the vertical tower configuration in Figure 50 with a resistivity of 150 ohm meter for short, medium, and long lines.

**Table 18 Results for Short Transmission Line**

<b>Calculation Method</b>	<b>Positive-Sequence Magnitude (Primary Ohms)</b>	<b>Positive-Sequence Angle (Degrees)</b>	<b>Zero-Sequence Magnitude (Primary Ohms)</b>	<b>Zero-Sequence Angle (Degrees)</b>
RTDS Simulation Values	5.684	84.885	21.195	72.173
Synchrophasor-Derived Values	4.358	69.463	21.753	69.446
Percent Error	23.329%	18.168%	2.633%	3.778%

**Table 19 Results for Medium Transmission Line**

<b>Calculation Method</b>	<b>Positive-Sequence Magnitude (Primary Ohms)</b>	<b>Positive-Sequence Angle (Degrees)</b>	<b>Zero-Sequence Magnitude (Primary Ohms)</b>	<b>Zero-Sequence Angle (Degrees)</b>
RTDS Simulation Values	28.418	84.885	105.974	72.173
Synchrophasor-Derived Values	22.115	68.997	107.89	69.557
Percent Error	22.180%	18.717%	1.808%	3.625%

**Table 20 Results for Long Transmission Line**

<b>Calculation Method</b>	<b>Positive-Sequence Magnitude (Primary Ohms)</b>	<b>Positive-Sequence Angle (Degrees)</b>	<b>Zero-Sequence Magnitude (Primary Ohms)</b>	<b>Zero-Sequence Angle (Degrees)</b>
RTDS Simulation Values	85.253	84.891	317.923	72.173
Synchrophasor-Derived Values	65.228	69.648	321.718	69.927
Percent Error	23.489%	17.956%	1.194%	3.112%

#### **4.6 Discussion and Summary of Results**

Figures 52 and 53 show a summary graph of the results for the untransposed transmission lines. In the case of untransposed lines for different tower configurations and ground resistivity, good results were obtained for the calculation of both positive- and zero-sequence impedances. The error did not exceed 5 percent. The exception is the vertical tower configuration for all line lengths. The error for both the positive-sequence magnitude and phase angle was high and identical around 20 percent. The zero-sequence parameters results were good and within 5 percent. Further investigation of the positive-sequence results revealed that the currents from the simulation software do not match the impedance matrix

(69) given by the program's line constants. Figure 54 shows A-phase current is the highest in magnitude; however, (69) shows the self-impedance for B-phase is the lowest and should yield the highest magnitude current. The synchrophasor-derived values calculated the actual impedance based on the currents injected, but compared to the actual line impedance entered in the program, they do not agree. Further investigation of the root cause of this discrepancy needs to be followed up on with the manufacturer of the software.

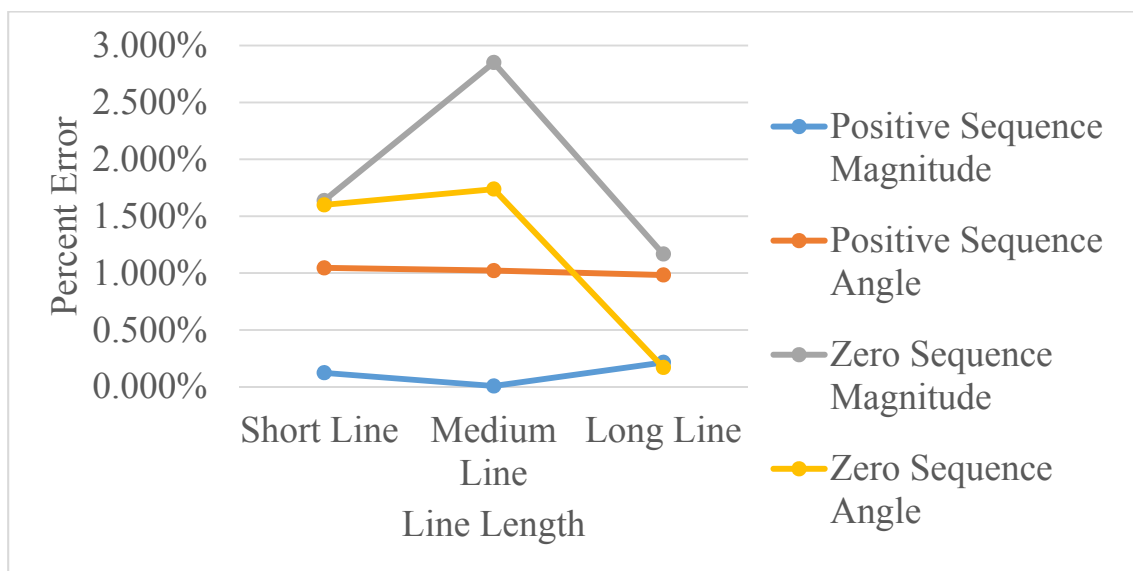


**Figure 53 Horizontal Tower Configuration Results**

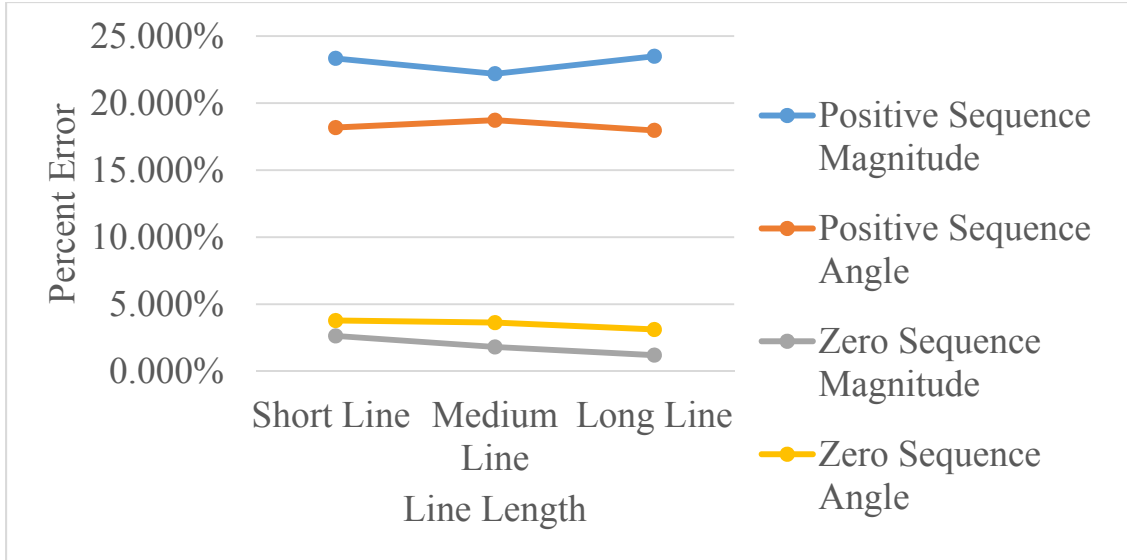


**Figure 54 Vertical Tower Configuration Results**

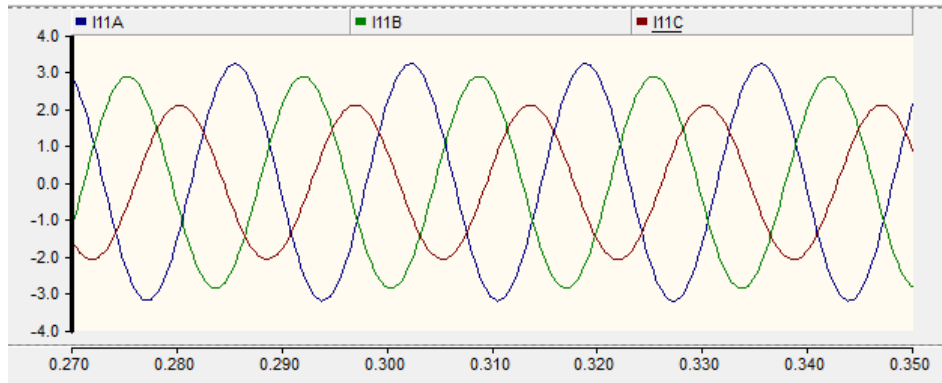


**Figure 55 PSCAD/EMTDC Simulation Results for Steady State Load Condition**

$$Z = \begin{bmatrix} 11.864+53.187i & 10.058+25.505i & 9.565+21.827i \\ 10.058+25.505i & 13.357+51.594i & 10.288+25.25i \\ 9.565+21.827i & 10.288+25.25i & 12.283+52.714i \end{bmatrix} \quad (69)$$



## Chapter 5 Measurement of Parallel Transmission Lines Parameters

### 5.1 Overview of the Calculation of Parallel Transmission Line Impedance

The concept of self and mutual impedances discussed in Chapter 2 for the derivation of the series impedance matrix  $Z$  and admittance matrix  $Y$  for three phase transmission lines can be extended to six conductors or more. Consider the case of two parallel transmission lines, as shown in Figure 56.

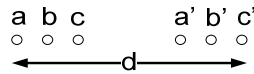


**Figure 56** Two Parallel Transmission Lines Separated by Distance  $d$

Equations (70) and (71) can be used to develop the series impedance matrix [11].

The series impedance is a 6x6 matrix.

$$Z = \begin{bmatrix} Z_{aa} & Z_{ab} & Z_{ac} & Z_{aa'} & Z_{ab'} & Z_{ac'} \\ Z_{ab} & Z_{bb} & Z_{bc} & Z_{bb'} & Z_{bb'} & Z_{bc'} \\ Z_{ac} & Z_{bc} & Z_{cc} & Z_{cb'} & Z_{cb'} & Z_{cc'} \\ Z_{aa'} & Z_{ba'} & Z_{ca'} & Z_{a'a'} & Z_{a'b'} & Z_{a'c'} \\ Z_{ab'} & Z_{bb'} & Z_{cb'} & Z_{a'b'} & Z_{b'b'} & Z_{b'c'} \\ Z_{ac'} & Z_{bc'} & Z_{cc'} & Z_{a'c'} & Z_{b'c'} & Z_{c'c'} \end{bmatrix} \quad (70)$$

And similarly the admittance matrix.

$$Y = \begin{bmatrix} Y_{aa} & Y_{ab} & Y_{ac} & Y_{aa'} & Y_{ab'} & Y_{ac'} \\ Y_{ab} & Y_{bb} & Y_{bc} & Y_{bb'} & Y_{bb'} & Y_{bc'} \\ Y_{ac} & Y_{bc} & Y_{cc} & Y_{cb'} & Y_{cb'} & Y_{cc'} \\ Y_{aa'} & Y_{ba'} & Y_{ca'} & Y_{a'a'} & Y_{a'b'} & Y_{a'c'} \\ Y_{ab'} & Y_{bb'} & Y_{cb'} & Y_{a'b'} & Y_{b'b'} & Y_{b'c'} \\ Y_{ac'} & Y_{bc'} & Y_{cc'} & Y_{a'c'} & Y_{b'c'} & Y_{c'c'} \end{bmatrix} \quad (71)$$

There are 21 unknowns in the series impedance matrix and 21 unknowns in the admittance matrix. In the case of transposed parallel transmission lines, the number of unknowns for both the series impedance and admittance matrix is reduced to seven as shown below

$$Z = \begin{bmatrix} Z_{self} & Z_{mutual1} & Z_{mutual1} & Z_{mutual1'} & Z_{mutual2'} & Z_{mutual3'} \\ Z_{mutual1} & Z_{self1} & Z_{mutual1} & Z_{mutual3'} & Z_{mutual1'} & Z_{mutual2'} \\ Z_{mutual1} & Z_{mutual1} & Z_{self1} & Z_{mutual2'} & Z_{mutual3'} & Z_{mutual1'} \\ Z_{mutual1'} & Z_{mutual3'} & Z_{mutual2'} & Z_{self2} & Z_{mutual2} & Z_{mutual2} \\ Z_{mutual2'} & Z_{mutual1'} & Z_{mutual3'} & Z_{mutual2} & Z_{self2} & Z_{mutual2} \\ Z_{mutual3'} & Z_{mutual2'} & Z_{mutual1} & Z_{mutual2} & Z_{mutual2} & Z_{self2} \end{bmatrix} \quad (72)$$

$$Y = \begin{bmatrix} Y_{self} & Y_{mutual1} & Y_{mutual1} & Y_{mutual1'} & Y_{mutual2'} & Y_{mutual3'} \\ Y_{mutual1} & Y_{self1} & Y_{mutual1} & Y_{mutual3'} & Y_{mutual1'} & Y_{mutual2'} \\ Y_{mutual1} & Y_{mutual1} & Y_{self1} & Y_{mutual2'} & Y_{mutual3'} & Y_{mutual1'} \\ Y_{mutual1'} & Y_{mutual3'} & Y_{mutual2'} & Y_{self2} & Y_{mutual2} & Y_{mutual2} \\ Y_{mutual2'} & Y_{mutual1'} & Y_{mutual3'} & Y_{mutual2} & Y_{self2} & Y_{mutual2} \\ Y_{mutual3'} & Y_{mutual2'} & Y_{mutual1} & Y_{mutual2} & Y_{mutual2} & Y_{self2} \end{bmatrix} \quad (73)$$

Once the admittance and series impedance matrices are determined, the symmetrical components transformation is applied to obtain the positive- and zero-sequence impedance of each transmission line as well as the mutual impedance terms.

The symmetrical impedance matrix is in the form:

$$Z_{012} = \begin{bmatrix} Z_0 & Z_{02} & Z_{01} & Z_{00'} & Z_{02'} & Z_{01'} \\ Z_{20} & Z_2 & Z_{21} & Z_{20'} & Z_{22'} & Z_{21'} \\ Z_{10} & Z_{12} & Z_1 & Z_{10'} & Z_{12'} & Z_{11'} \\ Z_{00'} & Z_{20'} & Z_{10'} & Z_{0'} & Z_2' & Z_{a'c'} \\ Z_{02'} & Z_{22'} & Z_{12'} & Z_{a'b'} & Z_2' & Z_{b'c'} \\ Z_{01'} & Z_{21'} & Z_{11'} & Z_{a'c'} & Z_{b'c'} & Z_1' \end{bmatrix} \quad (74)$$

From (74) the transmission line parameters can be extracted. The upper left 3x3 sub matrix is transmission line circuit 1 impedance terms. The bottom right 3x3 sub matrix is transmission line circuit 2 impedance terms. The zero sequence mutual coupling is  $Z_{00}$  shown on the first row.

The equivalent PI solution developed in Chapter 2 for untransposed lines will be used to solve for these matrices. Instead of 6 unknowns, now we have 21 unknowns in our equation (75).

$$V = Z \cdot I \quad (75)$$

## 5.2 PSCAD/EMTDC Simulation and Results

Figure 57 shows the simulation system in PSCAD/EMTDC for a 100 mile long untransposed parallel transmission line.

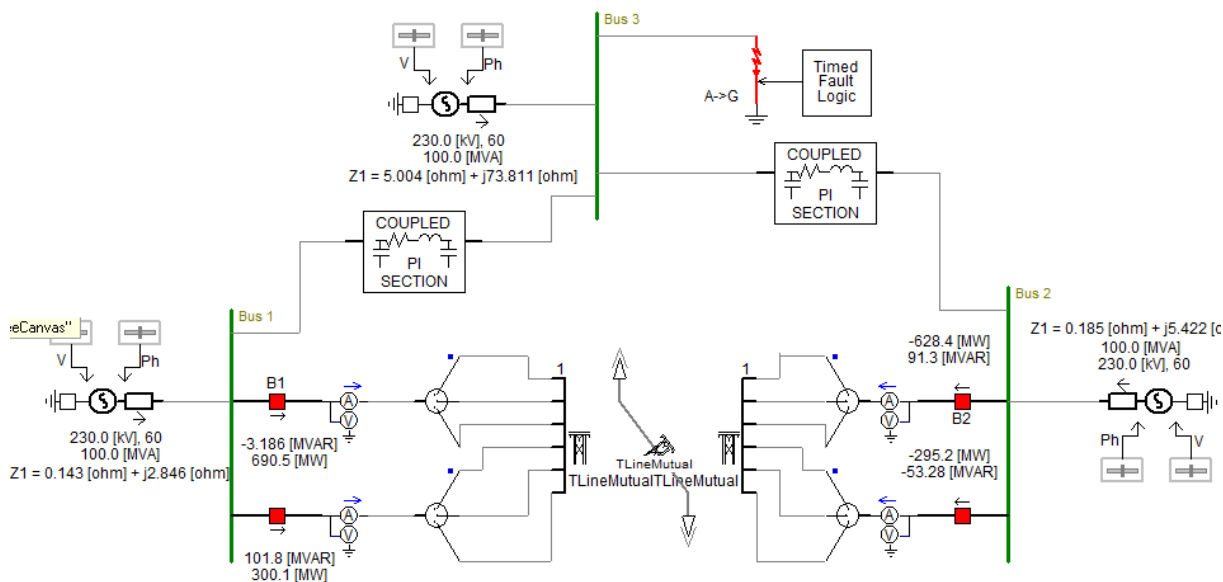


**Figure 57 PSCAD/EMTDC Set Up for Untransposed Parallel Transmission Line**

Because of the number of unknowns in the Y and Z matrices for parallel transmission lines, six independent states from the power system are needed to solve (64) and (65) shown in Chapter 2.

$$I = VY \quad (64)$$

$$V = Id \cdot Z \quad (65)$$

The conditions to solve (64) and (65) require (65) to have full rank. This can be achieved by having an open phase condition of each phase of each transmission line with a total of six open phase conditions as follows: A-phase open Line 1, B-phase open Line 1, C-phase open Line 1, A-phase open Line 2, B-phase open Line 2, and C-phase open Line 2.

Achieving these conditions in practice is challenging. This requires single pole breakers installed at both transmission lines to achieve these test conditions and willingness of the transmission line operators to conduct these tests.

The following tables provide the PSCAD/EMTDC results.

**Table 21 Transmission Circuit 1 Results**

<b>Calculation Method</b>	<b>Positive-Sequence Magnitude (Primary Ohms)</b>	<b>Positive-Sequence Angle (Degrees)</b>	<b>Zero-Sequence Magnitude (Primary Ohms)</b>	<b>Zero-Sequence Angle (Degrees)</b>
PSCAD/EMTDC Simulation Values	34.203	86.009	116.521	70.12
Synchrophasor-Derived Values	34.157	86.026	119.462	71.593
Percent Error	0.134%	0.020%	2.524%	2.101%

**Table 22 Transmission Circuit 2 Results**

<b>Calculation Method</b>	<b>Positive-Sequence Magnitude (Primary Ohms)</b>	<b>Positive-Sequence Angle (Degrees)</b>	<b>Zero-Sequence Magnitude (Primary Ohms)</b>	<b>Zero-Sequence Angle (Degrees)</b>
PSCAD/EMTDC Simulation Values	36.54	85.118	105.562	66.472
Synchrophasor-Derived Values	36.502	85.14	109.375	69.217
Percent Error	0.104%	0.026%	3.612%	4.130%

**Table 23 Zero-Sequence Mutual Coupling Results**

<b>Calculation Method</b>	<b>Zero-Sequence Magnitude (Primary Ohms)</b>	<b>Zero-Sequence Angle (Degrees)</b>
PSCAD/EMTDC Simulation Values	54.253	49.944
Synchrophasor-Derived Values	56.971	54.122
Percent Error	5.010%	8.365%

### 5.3 Relay Settings for Parallel Lines

Consider the configuration in Figure 58. The configuration is for parallel lines with common buses and is widely used for double-circuit towers that carry the lines from one bus to the other. In this parallel line application, the zero-sequence current of the parallel line flows into the line for remote ground faults, as illustrated in the figure. This causes an underreach of the zone distance relays. When  $I_{0p}$  is out of the line the distance relay will overreach [9].

One method to estimate the distance to the fault for A-phase-to-ground faults by mho elements was provided (66) in Chapter 3. The equation is modified to account for the mutual coupling, as shown in (76) [11].

$$m_{AG} = \frac{\operatorname{Re}(V_a \cdot V_{pol}^*)}{\operatorname{Re}\left(Z_{IL} \cdot \left(I_a + \left(\frac{Z_{0L} - Z_{1L} + Z_{0m}}{3Z_{L1}}\right) \cdot I_G\right) \cdot V_{pol}^*\right)} \quad (76)$$

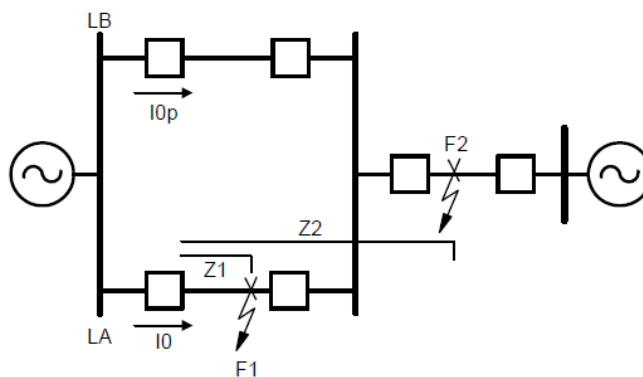


**Figure 58 Parallel Transmission Line System One Line**

The Zone 1 ground distance reach can be confidently set from 80 to 90 percent of the line because this independent zone will not overreach. The mutual effect of the parallel line will not allow Zone 1 to reach past F1. An overreach factor may be calculated for Zone 1, but the risk is to overreach when the parallel line has both of its terminals open. It is generally recommended to set the reach of Zone 1 like any other Zone 1 application. Overreaching zones, like Zone 2, should be compensated to make sure that the zero-sequence mutual does not reduce the desired reach. Overreaching zones are used in directional comparison systems (POTT, for example), and the relay settings should make sure that the overreaching zones reach past the remote terminal or more. For the F2 fault in Figure 58, both parallel lines carry the same direction and magnitude of zero-sequence current ( $I_0 = I_{0p}$ ), assuming the same transmission line impedance. The zero-sequence compensation factor without compensation for mutual coupling is:

$$k_0 = \frac{Z_{L0} - Z_{L1}}{3Z_{L1}} \quad (77)$$

For a parallel line application, therefore, the zero-sequence mutual coupling (78): [17]



$$k_{01} = \frac{Z_{L0} - Z_{L1} + Z_{0m}}{3Z_{L1}} \quad (78)$$

The  $k_0$  factor is the setting for the underreaching zone (Zone 1), and  $k_{01}$  is the setting for the overreaching zone (Zone 2). With this choice of  $k_0$  factors, it is acknowledged that the Zone 1 element may underreach but never overreach, and the Zone 2 element will always overreach the remote terminal with the appropriate reach. This is important for pilot relaying schemes that require overreaching zones for directional comparison schemes, like POTT. Another philosophy for parallel lines to ensure that Zone 2 will overreach is to extend the reach to a safe margin. Minimum settings of 120 to 150 percent are also used for this purpose.

The proposed method for checking relay settings demonstrated in Chapter 3 is still applicable for parallel lines. The addition of the  $k_{01}$  in (78) for overreaching zone distance elements includes the zero-sequence mutual coupling. The same criteria for the comparison between the line constants calculation and synchrophasors calculation can be used to check the settings for the overreaching compensation factor.

## Chapter 6 Conclusion and Future Work

### 6.1 Summary and Conclusion

Synchrophasor technology enabled us to gather power system data taken on a synchronized time schedule in multiple locations. This research presented an application of this technology to calculate the positive- and zero-sequence impedances for transposed and untransposed transmission lines. These calculations are used to verify distance relay settings. A review of transmission line parameters and modeling was presented.

The method used for the calculation of the positive- and zero-sequence impedances was demonstrated for both transposed and untransposed transmission lines. In the case of a transposed line, zero-sequence parameters were calculated from steady state load conditions if there is sufficient unbalance in the measured voltage. The minimum amount of unbalance required to perform the calculation was characterized. The equations to calculate the positive- and zero-sequence impedances and shunt admittances for a transposed line was shown if there is sufficient standing zero-sequence voltage unbalance during steady state.

In the case of untransposed lines or transposed lines without sufficient measured zero-sequence voltage unbalance, the parameters were calculated based on remote fault conditions involving ground in the system. These fault conditions were not necessarily on the line itself but could be anywhere that can generate enough zero-sequence unbalance. This unbalance was quantified.

In this research, field data from Entergy PMUs installed on a 230 kV untransposed transmission line was used to compare these calculations derived from synchrophasors with

the relay settings derived from line constants programs. A method for checking the relay settings was proposed based on the parameter calculations from the PMUs. The field data showed good results and further validated the proposed method.

Simulations using PSCAD/EMTDC software were used to validate the results and verify the accuracy and limitations of the calculation method.

The RTDS was used to further validate the performance in the presence of CTs and PTs and show the results from those calculations for different line length and tower configuration. The results from the RTDS confirmed the method used for the calculation and its accuracy.

Finally the calculation to parallel transmission lines was extended to calculate the zero-sequence mutual coupling in addition to both the positive and zero sequence impedance of each line. Recommendation for relay settings in the presence of mutual coupled lines was demonstrated. These recommendations can be used to verify or improve relay settings.

PSCAD/EMTDC was used to test the proposed calculation method and confirmed the results.

This research met the objective of demonstrating that synchrophasors can be used to calculate positive and zero sequence line parameters for both single lines and mutually coupled ones. It also provided the ability to verify or improve relay settings if the line impedance settings are incorrect.

## **6.2 Future Work**

- Series capacitors are introduced on transmission lines to increase power transfer capability and improve power system stability. These series compensated lines change the line impedance and present a challenge to setting distance relays. A proposed

research is to calculate the line parameters using synchrophasors for series compensated lines and provide a method to check the relay settings for these lines.

- The unbalanced states in the power system used in this research lasted longer than 3 cycles. This is typical for a transmission line breaker to clear a fault. The investigation and research to include unbalanced states that last a shorter duration is a topic of future research. The synchrophasor and field data in this research were collected at 30 messages per second. A higher collection rate may be needed in the case of faults cleared by fast fuses or fast breakers to make use of these unbalance conditions for the distance relay parameter verification.
- Another area of investigation is the sensitivity of PT errors on very short lines. Very short lines present a challenge to distance relays. In the case of very short lines, Zone 1 is sometimes turned off to avoid overreach or line differential protection is used instead. This investigation can shed some light on the limitation of this method if the line is too short.
- The method to calculate zero-sequence mutual coupling was presented for a double transmission line with a common bus. In the case of more than two parallel lines or lines that are parallel only certain distance away, the method for the calculation needs to account for the other lines as well. Also, how to validate the relay settings for those cases needs to be developed. For the case of zero-sequence mutual coupling, the limitation is that the method relies on opening single-pole breakers for the open-phase conditions. If the line only has three pole breakers, another method that relies on fault

conditions on the line needs to be investigated and required conditions to solve the mutual coupling needs to be developed.

- The method used field data from a single utility transmission line to validate the distance relay settings. More field data from single lines and parallel lines as well is needed to further compare the results of synchrophasor-derived values to actual relay settings. If there is a fault on the line with a known fault location, the performance of the relay can be evaluated to determine which method is more accurate.
- Tapped load on transmission lines can present a challenge to the proposed method to accurately measure the transmission line parameters. An area of investigation is to analyze the performance and perform testing with tapped load on transmission lines.
- This research used an offline software calculation to provide the relay settings checking method from the PMU inputs. One area of future work is to develop a hardware solution that can be implemented in the PMU or another processing device that can perform this validation in real time.

## References

- [1] D. Shi, D. J. Tylavsky, N. Logic, and K. M. Koellner, "Identification of Short Transmission-Line Parameters From Synchrophasor Measurements," proceedings of the 40th North American Power Symposium, Calgary, Canada, September 2008.
- [2] H. Z. Khorashadi and Z. Li, "A Novel PMU-Based Transmission Line Protection Scheme Design," proceedings of the 39th North American Power Symposium, Las Cruces, NM, September 2007.
- [3] K. Dasgupta and S. A. Soman, "Line Parameter Estimation Using Phasor Measurements by the Total Least Squares Approach," proceedings of the IEEE Power and Energy Society General Meeting, Vancouver, Canada, July 2013.
- [4] Z. Hu and Y. Chen, "New Method of Live Line Measuring the Inductance Parameters of Transmission Lines Based on GPS Technology," *IEEE Transactions on Power Delivery*, Vol. 23, Issue 3, July 2008, pp. 1288–1295.
- [5] S. E. Zocholl, "Sequence Components and Untransposed Transmission Lines." Available: [http://www.pacw.org/fileadmin/doc/Sequence\\_Components\\_Untransposed\\_Lines.pdf](http://www.pacw.org/fileadmin/doc/Sequence_Components_Untransposed_Lines.pdf), January 2014.
- [6] P. S. Meliopoulos, *Power System Grounding and Transients: An Introduction*. Marcel Dekker, New York, NY, 1988.
- [7] R. Bergen and V. Vittal, *Power Systems Analysis*. Prentice Hall, Upper Saddle River, NJ, 2000.
- [8] *PTC Mathcad User's Guide*. MathSoft, Inc., Cambridge, MA, 1999.
- [9] H. J. Altuve Ferrer and E. O. Schweitzer, III (eds.), *Modern Solutions for Protection, Control, and Monitoring of Electric Power Systems*. Schweitzer Engineering Laboratories, Inc., Pullman, WA, 2010.
- [10] Amberg, A. Rangel, and G. Smelich, "Validating Transmission Line Impedances Using Known Event Data," proceedings of the 65th Annual Conference for Protective Relay Engineers, College Station, TX, April 2012.
- [11] F. Calero, "Mutual Impedance in Parallel Lines – Protective Relaying and Fault Location Considerations," proceedings of the 34th Annual Western Protective Relay Conference, Spokane, WA, October 2007.

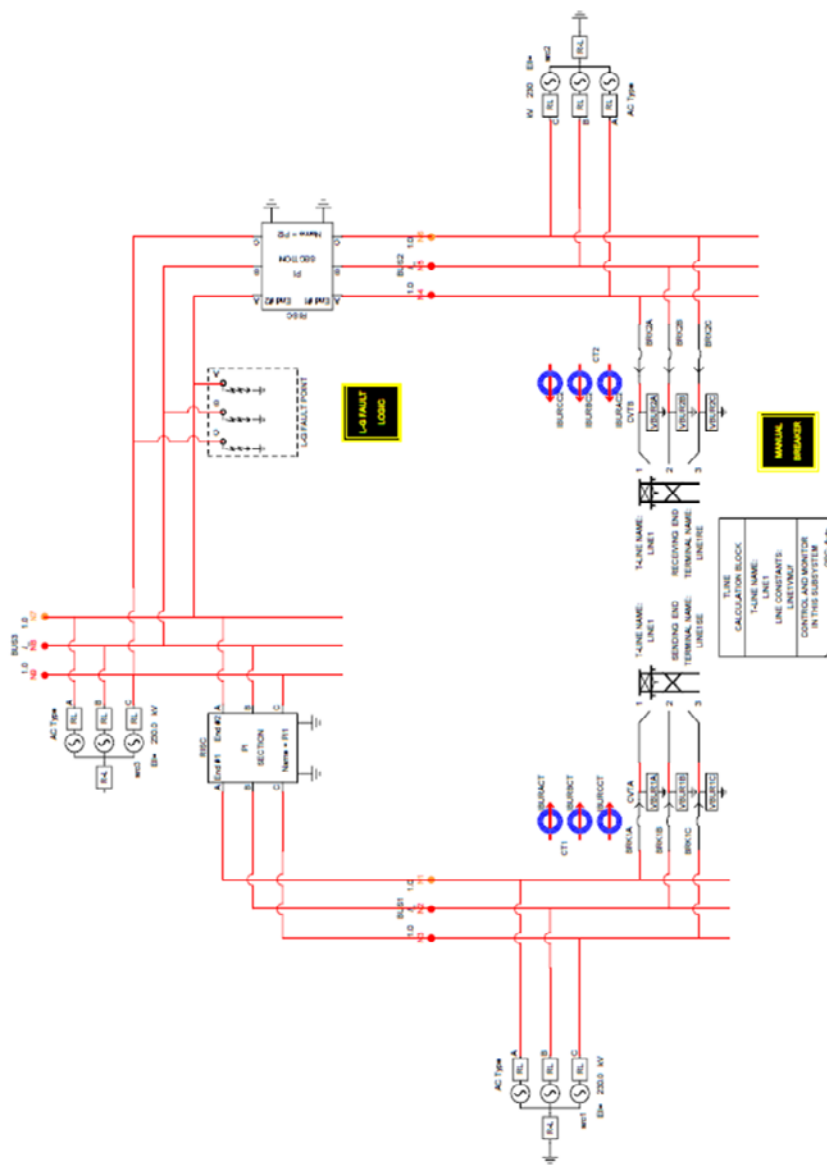
- [12] E&S Grounding Solutions, “What Is Soil Resistivity Testing?” Available: <http://www.esgroundingsolutions.com/about-electrical-grounding/what-is-soil-resistivity-testing.php>, November 2014.
- [13] United States Federal Communications Commission Encyclopedia, “M3 Map of Effective Ground Conductivity in the United States (A Wall Sized Map), for AM Broadcast Stations.” Available: <http://www.fcc.gov/encyclopedia/m3-map-effective-ground-conductivity-united-states-wall-sized-map-am-broadcast-stations>, November 2014.
- [14] J. R. Carson, “Wave Propagation in Overhead Wires With Ground Return,” *Bell System Technical Journal*, Vol 5, New York, 1926.
- [15] W. A. Elmore, “Zero Sequence Mutual Effects on Ground Distance Relays and Fault Locators,” proceedings of the 19th Annual Western Protective Relay Conference, Spokane, WA, October 1992.
- [16] SEL-421 Instruction Manual, Date Code 20130627. [Online]. Available: [http://www.selinc.com/instruction\\_manual.htm](http://www.selinc.com/instruction_manual.htm), June 2013.
- [17] J. Roberts and S. Turner, “Setting the Zero-Sequence Compensation Factors in SEL-321 Relays to Avoid Overreach in Mutual Coupled Lines,” SEL Application Guide AG98-03. [Online]. Available: <http://www.selinc.com/aglist.htm>, September 2014.
- [18] P. Kundur, *Power System Stability and Control*, 1ST edition. New York: McGraw-Hill Professional, 1994.
- [19] Solodov and V. Ochkov, *Differential Models: An Introduction with Mathcad*. Springer, Berlin, 2005.
- [20] *SEL-5073 Synchrowave Phasor Data Concentrator Instruction Manual*, SEL Inc., Pullman, WA.
- [21] *SEL-5078-2 Synchrowave Central Instruction Manual*, SEL Inc., Pullman, WA.
- [22] RTDS, RTDS Technologies Inc. Available: <http://www.rtds.com>, November, 2014.
- [23] Paul M. Anderson, *Analysis of Faulted Power Systems* (text), IEEE/Wiley Press, 1995.
- [24] H. Prado- Félix, V. Serna-Reyna, M, Mynam and A. Guzman, “Improve Transmission Fault Location and Distance Protection Using Accuarate Line Parameters,” proceedings of the 40th Annual Western Protective Relay Conference, Spokane, WA, October 2013.

- [25] SEL Inc, Synchrophasors Overview. Available:  
<https://www.selinc.com/synchrophasors/>, November, 2014.
- [26] RTDS Simulator Applications, RTDS Technologies Inc. Available:  
<http://www.rtds.com/applications/applications.html>, November, 2014.
- [27] “IEEE Standard for Synchrophasors for Power Systems,” *IEEE Std C37.118-2005*
- [28] “IEEE Standard for Synchrophasor Data Transfer for Power Systems,” *IEEE Std 37.118.2-2011*.



## Appendices

### Appendix A: Detail Circuit of the Power System Model



#### A.1 Source 1 Data

Source voltage = 230kV

Positive-sequence impedance = 2.85 ohms @ 87.12 degrees

Zero-sequence impedance = 1.299 ohms @ 83 degrees

### A.2 Source 2 Data

Source voltage = 230 kV

Positive-sequence impedance = 5.425 ohms @ 88 degrees

Zero-sequence impedance = 2 ohms @ 87 degrees

### A.3 Source 3 Data

Source voltage = 230 kV

Positive-sequence impedance = 73 ohms @ 86 degrees

Zero-sequence impedance = 76 ohms @ 81 degrees

### A.4 Current Transformer Data

PRE-PROCESSOR VARIABLE ( PPV ) SELECTION		PPV NAMES	PPV MAXIMUM VALUES		
V1,I1 ... V10,I10		P-LOSS DATA	MONITORING	SIGNAL NAMES	
MAIN DATA	PROCESSOR ASSIGNMENT	TRANSFORMER DATA		BURDEN	
Name	Description	Value	Unit	Min	Max
Rs	Secondary Side Resistance	0.84	Ohms	0.0	
Ls	Secondary Side Inductance	0	H	0.0	
Ratio	Turns ratio	400		0	

**Figure 59 CT Data**

## A.5 Potential Transformer Data

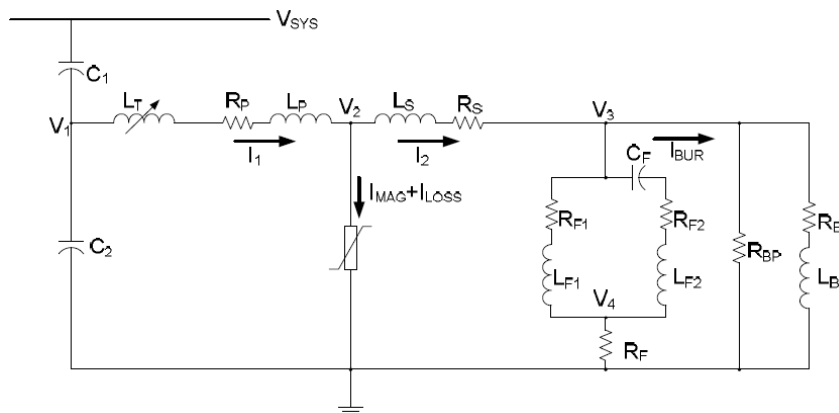


Figure 60 Equivalent CVT Model in RSCAD

If_rtds_sharc_slid_CVT1_VI					
P-LOSS DATA	MONITORING	SIGNAL NAMES			
FERRO-RESONANCE FILTER			B1,H1 ... B10,H10		
MAIN DATA	PROCESSOR ASSIGNMENT		TRANSFORMER DATA	BURDEN	
Name	Description	Value	Unit	Min	Max
Rp	Primary Side Resistance	474.0	Ohms	0.0	
Lp	Primary Side Inductance	4.46	H	0.0	
Np	Primary Side Turns	10713	turns	1	
Rs	Secondary Side Resistance	0.18	Ohms	0.0	
Ls	Secondary Side Inductance	0.47e-3	H	0.0	
Ns	Secondary Side Turns	115	turns	1	

Figure 61 CVT Transformer Data

If_rtds_sharc_slid_CVT1_VI					
P-LOSS DATA	MONITORING	SIGNAL NAMES			
FERRO-RESONANCE FILTER			B1,H1 ... B10,H10		
MAIN DATA	PROCESSOR ASSIGNMENT		TRANSFORMER DATA	BURDEN	
Name	Description	Value	Unit	Min	Max
Rb	Burden series resistance	400.9	Ohms	0.0	
Lb	Burden series inductance	1.84	H	0.0	
Rbp	Burden parallel resistance	2298.0	Ohms	0.0	

Figure 62 CVT Burden Data

If_rtds_sharc_slid_CVT1_VI					
P-LOSS DATA		MONITORING		SIGNAL NAMES	
FERRO-RESONANCE FILTER				B1,H1 ... B10,H10	
MAIN DATA		PROCESSOR ASSIGNMENT		TRANSFORMER DATA	
				BURDEN	
Name	Description	Value	Unit	Min	Max
Rf1		1.06	Ohms	0.0	
Lf1		0.01	H	0.0	
Cf		8.0	uF	0.0	
Rf2		4.24	Ohms	0.0	
Lf2		0.394	H	0.0	
Rf		40.0	Ohms	0.0	

**Figure 63 CVT Ferro-Resonance Filter Data**

## Appendix B: Solving a System of Linear Equations

### B.1 Mathcad Isolve and geninv functions

$\text{Isolve}(M, v)$  Returns the solution  $x$  for the linear system of equations  $M \cdot x = v$ , using LU decomposition. In the case of an inconsistent system of equations,  $\text{Isolve}$  returns the least-squares solution, given also by  $\text{geninv}(M) \cdot v$ .

$\text{geninv}(A)$  Returns  $L$ , the generalized (pseudo) inverse of  $A$ , which gives the least-squares solution to a system of equations. If  $x = L \cdot b$ , then  $x$  is the minimum of  $|A \cdot x - b|^2$ . If  $A$  is square, and nonsingular, then  $\text{geninv}$  returns  $A^{-1}$ .

If there is a small measurement error such as:

$$B = A x + \text{Error} \quad (79)$$

Where:

$B$  is the voltage measurement matrix.

$A$  is the current measurement matrix.

Error is  $Ax - b$ .

The least-square solution is to minimize (78), which is the residual or the error. This accounts for error in the current measurement but not the voltage measurement.